Role of alkali field strength on the speciation of Ni2+ in alkali borate glasses: comparison with crystalline Ni-borates

Laurence Galoisy, Georges Calas

Role of alkali field strength on the speciation of Ni^{2+} in alkali borate glasses: comparison with crystalline Ni-borates

Laurence Galoisy, Georges Calas

Sorbonne Université, CNRS, Muséum National d'Histoire Naturelle, Institut de Minéralogie, de Physique des Matériaux et de Cosmochimie (IMPMC), IRD, 75005 Paris, France

**Corresponding author: laurence.galoisy@sorbonne-universite.fr (L. Galoisy).*

ABSTRACT

This work presents a comparative spectroscopic study of Ni speciation in binary alkali borate glasses, with up to 35 mol% alkali oxides, using optical absorption spectroscopy and Ni K-edge X-ray Absorption Near Edge Structure (XANES)- and taking advantage of comparison with previous structural information obtained with Ni K-edge Extended X-ray Absorption Spectroscopy (EXAFS) on the same samples. Nickel-bearing K, Na or Li borate glasses exhibit an exceptional diversity of coloration (from green to yellow, brown, and purple). This is due to a progressive coordination change of Ni^{2+} with increasing alkali content, from 6-, to 5- and 4-Ni-coordination, each coordination state having a peculiar structural significance. $^{[6]}Ni^{2+}$ is predominant in low alkali borate glasses, where Ni octahedra cluster in ordered Ni-rich domains. $^{[4]}Ni^{2+}$ is formed at low alkali cation field strength: it predominates in high potassic glasses but it is only a minor coordination state in Na-borate glasses and it is absent in Li-borate glasses, in which, by contrast, $^{[5]}Ni^{2+}$ prevails. For these three coordination states, the comparison with the structure of crystalline borates suggests a diversity of linkages between Ni^{2+} and the borate polymeric network. Among the alkali borate glasses investigated, each Ni-coordination state shows similar spectroscopic properties. This implies that the modification of Ni speciation with glass composition arises only from a variation of the relative contribution of 6-, 5- and 4-coordinated Ni^{2+} without significant modification of the spectroscopic parameters characteristic of each site. The coordination number of Ni^{2+} is correlated with the field strength of the modifier cations present in the glass: higher the field strength of the modifier cations, higher the nickel coordination number. High-K borate glasses favor the formation of $^{[4]}Ni^{2+}$, as

this coordination state is not observed in Li- and is only minority in Na borate glasses, because of Li and Na preference for charge compensating $^{[4]}B$ instead of $^{[4]}Ni^{2+}$. Due to the similarities between Ni^{2+} and Mg^{2+}, the diversity of the structural scenarios around Ni^{2+} in alkali borate glasses may shed light on the structural behavior of Mg in the same glasses, providing additional evidence of the control of Mg coordination by the field strength of the alkalis.

Keywords: borate glasses; glass structure; UV-visible spectra; XANES spectra; crystalline borates; Mg coordination.

1. Introduction

Alkali borate glasses exhibit an original structure based on the complex interplay between three- and four-coordinated boron (referred to as $^{[3]}B$ and $^{[4]}B$, respectively). Alkali elements are able to charge compensate the charge deficit of $^{[4]}B$ or to depolymerize the borate network by generating non-bridging oxygen atoms. By contrast to most glasses, which are considered to have only a short range ordered structure, these glasses show a crystal-like medium range order in alkali-poor compositions, due to the presence of rigid super-structural units based on an interlinkage between $^{[3]}B$ and $^{[4]}B$ sites [1]. The coordination change from $^{[3]}B$ to $^{[4]}B$ with increasing alkali content modifies the structural properties of the other glass components, as alkali ions associated to B turn from a modifying to a charge-compensating role. As a consequence, alkali borate glasses exhibit important modifications of their structure, properties and dynamics as a function of the cation content and field strength.

It has long been observed that the presence of transition elements in glasses causes spectacular color changes with or without any modification of their oxidation state [2-4]: in alkali borate glasses, transition elements are at the origin of one of the most noticeable chemical dependence of the color of oxide glasses. For instance, Ni^{2+} in potassium borate glasses gives rise to colors that vary from green to yellow to brown and to purple with increasing potassium content. This color change corresponds to a decrease of the coordination number of Ni^{2+} from 6 to 5 and 4 with increasing alkali levels. A low field strength of alkalis plays a major role in enhancing the conversion to $^{[4]}Ni^{2+}$ as also observed in silicate glasses [5]. A similar behavior has been shown

in cobalt-bearing alkali borate glasses [6], with a similar decrease in the coordination number of Co^{2+} from 6 to 5 and 4 with increasing alkali levels and a low cation field strength favoring $^{[4]}Co^{2+}$. Similarly, the coordination number of uranyl groups in Li borate glasses decreases in $30Li_2O$-$70B_2O_3$ borate glasses relative to $10Li_2O$-$90B_2O_3$ glasses, with 5 and 6 equatorial oxygen ligands, respectively [7].

Alkali borate glasses show a more complex evolution of Ni^{2+} coordination with glass composition than alkali silicate glasses [8]: at low alkali content, borate glasses are the only Ni-bearing oxide glasses to exhibit a green color, indicative of the octahedral coordination of Ni^{2+}. Extended X-ray Absorption Spectroscopy (EXAFS) demonstrated that these octahedral sites occur in ordered defective domains [9,10]. With increasing alkali content, these nanodomains progressively disappear, in relation with a coordination change of $^{[6]}Ni^{2+}$ to $^{[5]}Ni^{2+}$ and $^{[4]}Ni^{2+}$ [11]. Until now, most studies have discussed Ni^{2+}-coordination in alkali borate glasses on the only basis of Ni^{2+} crystal field spectra [4, 12]. The present study provides a new interpretation of optical absorption spectroscopic properties of Ni^{2+} in alkali (Li, Na, K) borate glasses, with an alkali content ranging from 10 to 35 mol%. These data are compared to Ni-bearing crystalline borates. Complementary structural information is obtained from Ni K-edge X-ray absorption near edge structure (XANES) spectroscopy. We also use previous EXAFS data obtained on the same glasses [11]. We confirm the presence of $^{[5]}Ni^{2+}$ as in most oxide glasses [5], in addition to $^{[4]}$- and $^{[6]}Ni^{2+}$, the proportion between these different coordination states being dependent on glass composition. The use of these complementary techniques allows reject some exotic coordination states invoked in the past, such as square-planar, 8- or 12-fold coordinated Ni^{2+}. The relative proportion of $^{[4]}$-, $^{[5]}$- and $^{[6]}Ni^{2+}$ is composition dependent and is responsible for the coloration of Ni^{2+}-bearing alkali borate glasses.

2. Experimental methods

2.1. Glass synthesis

Li, Na and K borate glasses have been prepared by melting appropriate amounts of dried high purity grade K_2CO_3, Na_2CO_3, Li_2CO_3 and H_3BO_3. Starting reagents were Li_2CO_3 (Merck, 99%), Na_2CO_3 (Merck, 99.5%), K_2CO_3 (Merck 99%) and B_2O_3 (Aldrich, 99.98%). Nickel was introduced as NiO (Merck, 99.9%). After

decarbonation at 750°C, the compositions were melted in a Pt crucible at 1100°C during 4 hours to limit alkali losses. The glasses were quenched by pouring onto a metallic plate to obtain high quench speed giving plates with parallel faces of about 0.5 mm thickness and a few cm diameter. They were not annealed. Low alkali borate glasses were kept in vaseline oil to prevent glass hydration during exposure to air, particularly with less than 20 mol% alkali oxides. To minimize the effect due to the hydroscopic nature of these samples, the optical spectra data were recorded as quickly as possible after synthesis. Special care was given to the synthesis of samples low in network modifiers, which may show the presence of some unfused NiO due to the low solubility of NiO causing light scattering in these compositions [13]. The absence of light scattering effects in the optical absorption spectra demonstrates that NiO is well dissolved of our samples.

The amorphous nature of the glasses was checked by x-ray diffraction. The actual composition of the glasses was obtained by flame Atomic Absorption Spectroscopy for boron and alkalis (within ± 1 %) and by electron microprobe for Ni (within 0.05% after averaging 10 analytical points) using the Cameca microbeam Microprobe of the Camparis analytical facility of Sorbonne University. Glass composition, normalized to 100 mol%, is given in Table 1 with nominal composition in brackets. The glasses appear visually homogeneous, transparent, with a constant coloration.

	B_2O_3	Li_2O	Na_2O	K_2O	NiO
LiB10	88.1 (90)	10 (10)			1.9 (2)
LiB20	79 (80)	19.3 (20)			1.7 (2)
LiB30	69 (70)	29.2 (30)			1.8 (2)
NaB10	89.8 (90)		8.8 (10)		1.4 (2)
NaB20	79.5 (80)		20 (20)		1.5 (2)
NaB30	69.5 (70)		28.8 (30)		1.7 (2)
KB10	87.1 (90)			11.4 (10)	1.5 (2)
KB20	80.3 (80)			18 (20)	1.7 (2)

KB27	71.1 (73)	27 (27)	1.9 (2)
KB31	67 (69)	31.2 (31)	1.8 (2)
KB35	63 (65)	35.1 (35)	1.9 (2)

Table 1: Chemical composition of the alkali borate glasses investigated (mol%). The nominal compositions are given in brackets.

2.2. Crystalline references

Crystalline $CaNiSi_2O_6$ was used as a reference for slightly distorted $^{[6]}Ni^{2+}$ [14] and $NiCr_2O_4$ and Ni-bearing ß-Al_2O_3 for $^{[4]}Ni^{2+}$ [15]. $KNiPO_4$ and α-$Ni_2P_2O_7$ were used as a reference for $^{[5]}Ni^{2+}$in a square pyramid geometry and coexisting $^{[6]}$- and $^{[5]}Ni^{2+}$in a trigonal bipyramid symmetry, respectively [8]. The synthesis conditions of these crystalline references and their spectroscopic properties have already been reported [8, 14, 15].

2.3. Optical absorption spectroscopy

Crystal field transmission spectra of parallel polished plates of glasses have been recorded at room temperature between 250 to 2500 nm, with an UV-Visible-NIR computerized 2300 CARY spectrophotometer. After conversion of wavelengths into wavenumbers, a baseline correction was performed to account for the physical processes superimposed to electronic intraconfigurational transitions (coherent light scattering, ligand-to-metal charge transfer transitions).

Diffuse reflectance spectroscopy was used for the crystalline references, using a 9-inch-diameter integrating sphere coated with halon. These samples were prepared as finely ground powders deposited on Al sample holders. Diffuse reflectance values were obtained by reference to halon. Reflectance values (R) are converted into a remission function F(R) using the Kubelka-Munk formalism:

$$F(R) = (1 - R^2)/2R.$$

F(R) is a good approximation of the absorbance of a light scatterer of infinite thickness [16]. We first removed the background of the crystal field spectra obtained either in the diffuse reflectance mode or in transmission. We fitted the spectra (in a wavenumber scale, proportional to energy) into Gaussian components

using a home made software to determine the transitions responsible for the various absorption bands, as already discussed for Ni-bearing minerals [8,16].

2.4. X-ray absorption spectroscopy

X-ray Absorption Spectroscopy (XAS) experiments at the Ni K-edge were performed on the D44 station at the LURE-DCI synchrotron source (Orsay, France). The storage ring was operating at 1.85 GeV positron energy and 200mA positron current. XAS spectra were collected in transmission mode and sample thickness was optimized to get an absorption step between 0.5 and 1. The X-ray detectors were ionizing chambers filled with air.

XANES (X-ray absorption near edge structure) spectra were recorded at room temperature and collected from 8200 to 8600 eV using a Si (311) double-crystal monochromator, which provides a spectral resolution of 1.9 eV. The energy steps were 0.15eV for the pre-edge region and 0.5 eV for the main part of the edge, with 3sec accumulation time. Energy calibration was repeatedly checked by recording metallic Cu reference spectra after every three measurements and is accurate within 0.3 eV. The XANES spectra have been normalized to the atomic absorption above the absorption threshold, extracted by a polynomial fit. First and second derivative functions were used to determine the exact position of the various XANES features. Pre-edge features have been extracted after main-edge background removal, using an arctangent function.

3. Results

3.1. XANES

3.1.1. Crystalline references

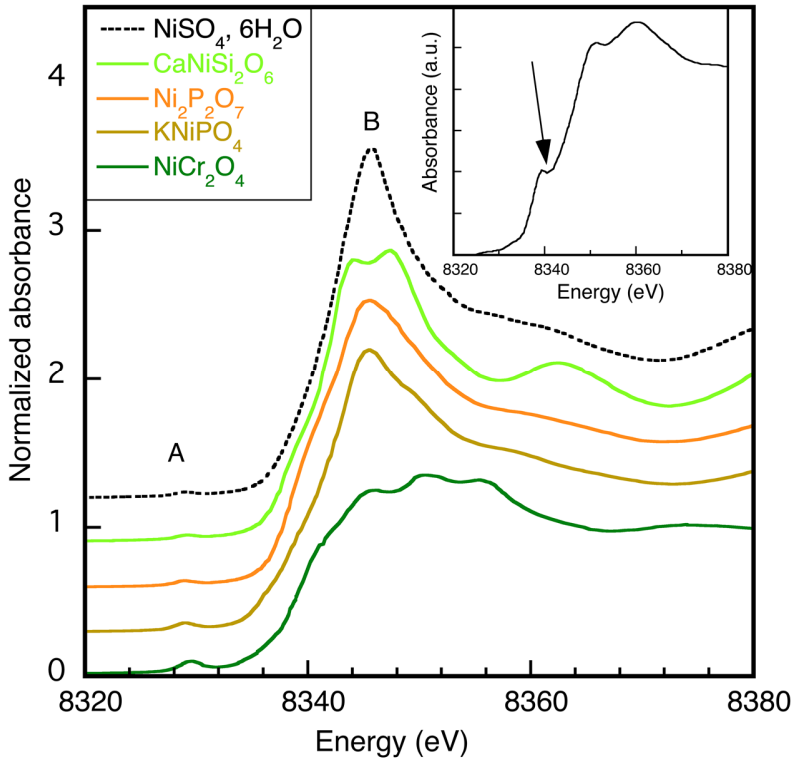

Fig. 1. Normalized Ni-K edge XANES spectra of crystalline references: [6]$NiSO_4$, $6H_2O$ and Ca[6]$NiSi_2O_6$, K[5]$NiPO_4$ and [4]$NiCr_2O_4$. Ni^{2+} occurs in 6- and 5 coordination in α–$Ni_2P_2O_7$. The two regions A and B represent the pre-edge and main edge resonance, respectively. The inset represents the XANES spectrum of a Ni^{2+} square planar complex, which shows the characteristic signature of this coordination state (arrow) (after [17], modified). This diagnostic feature is not observed in the XANES spectra of alkali borate glasses.

Reference compounds were chosen to correspond to the most probable coordination numbers of Ni^{2+} in borate glasses: regular and distorted octahedral site in $NiSO_4$, $6H_2O$ and $CaNiSi_2O_6$, respectively; square pyramid site in $KNiPO_4$ ($C4_V$ site symmetry) and tetrahedral site in [4]$NiCr_2O_4$. Ni^{2+} occurs in both 6- and 5 coordination (trigonal bipyramid site with a $D3h$ site symmetry) in α–$Ni_2P_2O_7$. The two regions of the XANES spectra, the pre-edge (A feature) and the main edge (B feature), show an evolution of their relative intensity and lineshape as a function of Ni^{2+} coordination geometry (**Fig. 1**). The A feature corresponds to electronic transitions from the *1s* core-level to the *3d* empty orbitals and is quadrupolar and parity forbidden. As a consequence, it is enhanced by an increased *p* character of the final state, such hybridization being favored in

the absence of an inversion center [18]. The pre-edge intensity increases from 6- to 5-and 4-coordinated Ni. The B Feature is ascribed to dipolar transitions to empty *4p* states superimposed to multiple scattering resonances. As it results from the transition to the *p* empty density of state of the absorber, it is influenced by the *sp* hybridization of the oxygen neighbors and an increased hybridization decreases the *p* character of the final state. This causes the intensity of the B feature to decrease from 6- to 5- and 4-coordinated Ni^{2+}.

The sharpest B feature occurs in the spectrum of $^{[6]}NiSO_4$, $6H_2O$, in agreement with a regular geometry of the octahedral Ni-site. It is split by 2.8 eV in $Ca^{[6]}NiSi_2O_6$, consistent with a distortion of the Ni^{2+} site. The lowest intensity of the B feature is observed in the spectrum of $NiCr_2O_4$, the spectra of the $^{[5]}Ni^{2+}$compounds showing an intermediate intensity. The lowest intensity of the A feature is found in a pure octahedral symmetry as in $NiSO_4$, $6H_2O$ and it increases with the hybridization of the Ni^{2+} *3d* and *4p* orbitals in non-centrosymmetric sites, which is observed for $^{[4]}Ni^{2+}$ in $NiCr_2O_4$. As for the B feature, the intensity of the A feature for $^{[5]}$Ni is intermediate relative to that of $^{[4]}$- and $^{[6]}Ni^{2+}$compounds. Finally, a square planar environment gives rise to a characteristic Ni ($1s \rightarrow 4p_z$) transition superimposed to the rising main edge (inset, **Fig. 1**). The absence of this peculiar feature allows reject such Ni coordination state in alkali borate glasses (see 3.1.2).

3.1.2. Borate glasses

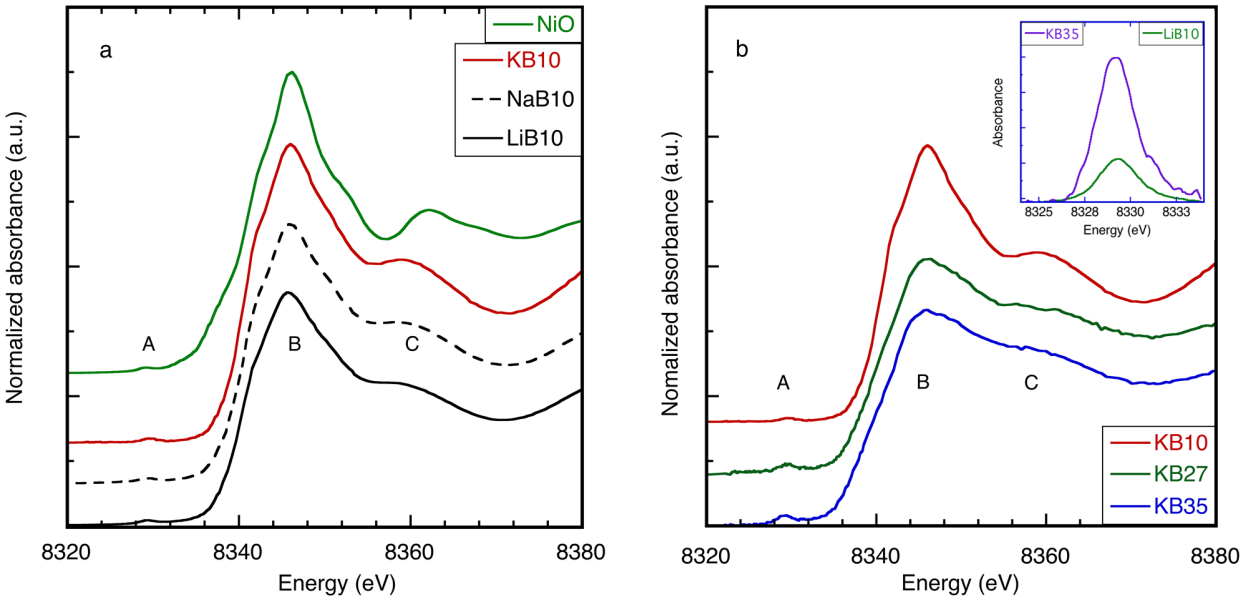

Fig. 2. Normalized Ni-K edge XANES spectra of alkali borate glasses. **a.** Comparison between glasses with 10 mol% alkali (LiB10, NaB10, KB10) and NiO; **b.** Comparison between glasses with 10%, 27% and 31%

179 K_2O (KB10, KB27, KB35). The inset shows the increase of the intensity of the Ni pre-edge between LiB10
180 ($^{[6]}Ni^{2+}$) and KB35 ($^{[5]-}$ and $^{[4]}Ni^{2+}$) glasses.
181
182 The XANES spectra of LiB10, NaB10 and KB10 glasses (**Fig. 2a**) are almost identical. The low intensity
183 of the pre-edge feature (A) indicates a regular octahedral coordination, as in nickel sulfate, $NiSO_4$, $6H_2O$ (**Fig.**
184 **1**). These spectra are different from the XANES spectrum of NiO [19]. It exhibits a characteristic main edge (B)
185 rising at lower energy than in the glasses due to O to Ni charge-transfer processes, the appearance of new
186 features at 8337 eV and 8352 eV and a shift of the multiple scattering XANES resonance (C) from 8358 to 8362
187 eV. These differences in the XANES spectra are a confirmation that the ordered defective NiO-like domains
188 evidenced by EXAFS in these glasses [9,10] do not correspond to unreacted NiO crystallites.
189 From KB10 to KB27 and KB35 (**Fig. 2b**), the intensity of the pre-edge (A) increases and that of the main
190 edge (B) decreases, as observed in $^{[4]}Ni^{2+}$ vs. $^{[6]}Ni^{2+}$ references. The XANES spectra of NaB30 show a pre-edge
191 intensity close to that of KB35. This is consistent with a transformation of Ni^{2+} sites from a regular octahedral
192 coordination to non-centrosymmetric sites at increasing alkali content. Features B and C are well structured for
193 KB10 but become broader for KB27 and KB35, as a result of Ni^{2+}- site distribution. Finally, none of the
194 investigated spectra shows the presence of the Ni ($1s \rightarrow 4p_z$) transition characteristic of a square-planar
195 geometry as observed in the XANES spectra of Ni^{2+} square-planar complexes (**Fig. 1**) [17].
196
197 *3.2. UV-visible-near IR absorption spectroscopy*
198
199 *3.2.1. Crystalline references*

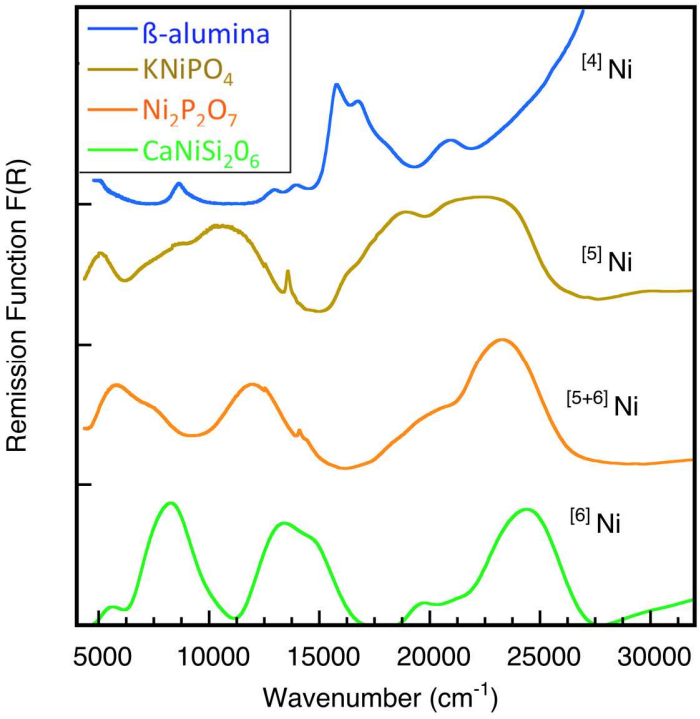

Fig. 3. Remission function F(R) of Ni-bearing crystalline references: $Ca^{[6]}NiSi_2O_6$, □α-$^{[5+6]}Ni_2P_2O_7$, $K^{[5]}NiPO_4$ and ß-Al_2O_3:$^{[4]}$Ni. This function is a good approximation of sample absorbance in the Kubelka-Munk formalism (see 2.3).

Octahedral Ni^{2+} is characterized by three spin allowed transitions at 8280 cm^{-1} (crystal field transition), 13170 cm^{-1} and 24450 cm^{-1} in $CaNiSi_2O_6$ (**Fig. 3**). These transitions correspond to a crystal field splitting $10Dq$ = 8280 cm^{-1} and a Racah parameter B = 890 cm^{-1} (the free ion value is B=1030 cm^{-1}) [14]. The crystal field transition bears a Gaussian shape with a full linewidth of 2700 cm^{-1}, due to a low distortion of the $^{[6]}Ni^{2+}$-site. Spin-orbit coupling effects enhance the intensity of the spin-forbidden transitions to $^1E_g(D)$ and $^1A_{1g}$ (G) levels at 14900 and 19670 cm^{-1}, respectively.

The absorption bands of $^{[4]}Ni^{2+}$ observed in ß-Al_2O_3 are shifted to lower wavenumber values relative to $^{[6]}Ni^{2+}$. They occur near 5000, 8500 and 15500 cm^{-1} [15]. Site distortion (Jahn-Teller effect) and spin-orbit coupling cause the splitting of the 15500 cm^{-1} transition. The characteristic field-independent spin forbidden transitions at 13000 and 13900 cm^{-1} retain a narrow lineshape in the optical spectra of $^{[4]}Ni^{2+}$.

The crystal field spectra of $^{[5]}Ni^{2+}$ present a higher number of allowed optical transitions (five and six in

Trigonal bipyramid (TBP) and Square pyramid (SP) configurations, respectively) than in octahedral or tetrahedral coordination [20]. In $KNiPO_4$, the broad band near 10000 cm^{-1} arises from partly overlapping absorption bands. As a consequence, the two absorption bands occurring at low wavenumbers have different linewidths in $^{[5]}Ni^{2+}$ by contrast to $^{[6]}Ni^{2+}$ in which the linewidths are similar. The most intense absorption band occurs at a position intermediate between that in $^{[6]}$- and $^{[4]}Ni^{2+}$, near 22000 cm^{-1} with a shoulder near 19000 cm^{-1}. A characteristic narrow spin-forbidden transition is observed at 13900 cm^{-1} as in crystalline phosphates and borates [13, 19, 21]. The spectrum of α-$Ni_2P_2O_7$ [15] is remarkably similar to that of $MgNiP_2O_7$ [22]. The position of the main absorption bands is shifted relative to the spectrum of $KNiPO_4$, due to a different geometry of the $^{[5]}Ni^{2+}$ square pyramidal site. However, square pyramid and trigonal bipyramid sites may mutually transform easily, which makes it difficult to decipher among these two geometries. An important spectroscopic property of Ni^{2+} is that the most intense absorption bands are redshifted with decreasing Ni-coordination number. This is consistent with a crystal field intensity decreasing with the number of ligands.

3.2.2. Borate glasses

The optical spectra of alkali borate glasses (**Fig. 4**) show dramatic differences as a function of the alkali content, at the origin of well-known spectacular color variations [2-4]. All spectra lie on a horizontal background. The values of the molar extinction coefficient ε found in this study are similar to those of the literature [2-4]. The nature of the alkali directly influences the chemical dependence of glass color and hence the shape of the optical absorption spectra, an indication of a coordination change of Ni^{2+}. Glasses with low and intermediate Li or Na content are green and brown, respectively. Glasses with high potassium content are purple, while glasses with a high Li or Na content remain brown.

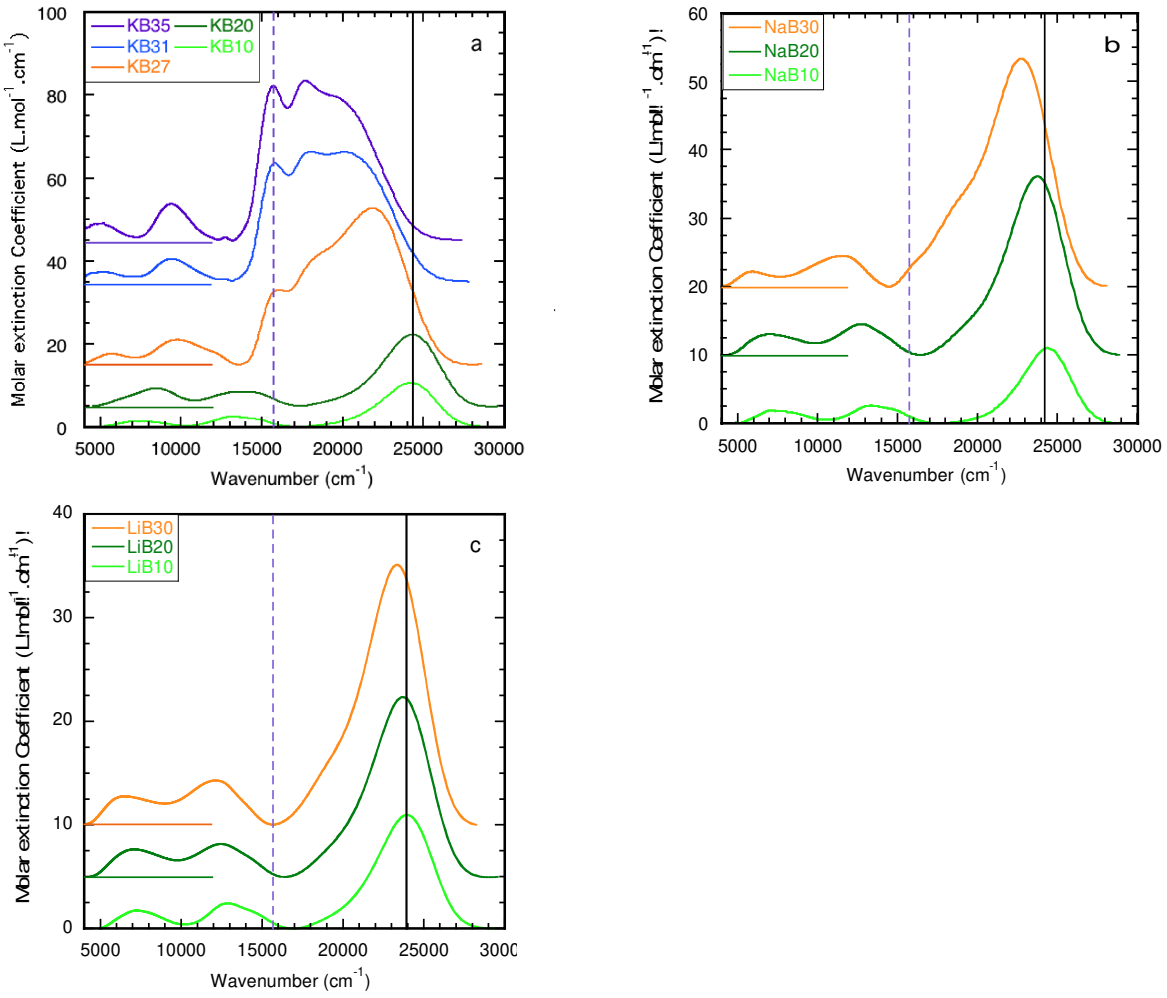

Fig. 4. Optical absorption spectra of Ni^{2+} in **a.** K-borate glasses, **b.** Na-borate glasses, **c.** Li-borate glasses. The position of the characteristic transitions of octahedral and tetrahedral Ni^{2+} is represented by a full and a dashed line, respectively, as a guide for the eye, to appreciate the modification of the position of the main absorption bands. The position of the main band for $^{[5]}Ni^{2+}$ occurs at lower wavenumbers (22000-23000 cm^{-1}) as compared to $^{[6]}Ni^{2+}$ (24000-25000 cm^{-1}).

The spectra of the KB10 (**Fig. 4a**), NaB10 (**Fig. 4b**) and LiB10 (**Fig. 4c**) glasses are almost identical and show similar decomposition into Gaussian components (**Fig. A1**). These spectra characterize the presence of $^{[6]}Ni^{2+}$ as recognized in previous studies [2-4]. The green color of these glasses is a visual indication that the $^{[6]}Ni^{2+}$ sites are not significantly distorted. Indeed, distorted $^{[6]}Ni^{2+}$ sites are known to impart a yellow color in crystalline materials, due to a splitting of the main band that causes a modification of the transmission window

249 [23]. The spectra do not show the presence of light scattering, assigned in other studies (see 2.1) to unreacted
250 NiO [13].

251 In K-borate glasses (**Fig. 4a**), the optical spectra show dramatic changes in relation with the appearance
252 of different Ni-coordination sites. The dashed vertical line corresponds to the contribution of tetrahedral $Ni^{2+,}$
253 showing that the position of the main $^{[4]}Ni^{2+}$ absorption band remains stationary. The absorbance value at this
254 position dashed line allows assess the progressive increase of the proportion of $^{[4]}Ni^{2+}$ with increasing K-content
255 from KB27 to KB35. The whole absorption spectrum is affected by the progressive domination of the
256 tetrahedral Ni^{2+} transitions at increasing potassium content. In the KB27 glass, showing a deep brown color, the
257 most intense transition occurs near 22000 cm^{-1}. However, in addition to this absorption band characteristic of
258 $^{[5]}Ni^{2+}$, the spectrum is characterized by the presence of a band near 15600 cm^{-1}, diagnostic of the $^3T_1(F) \rightarrow$
259 $^3T_1(P)$ transition of $^{[4]}Ni^{2+}$. The band near 5000 cm^{-1} has a Gaussian shape (**Fig. A3**) and corresponds to the
260 $^{[4]}Ni^{2+}$ crystal field transition. The color of the KB31 and KB35 glasses is purple: the transmission window is
261 redshifted towards lower wavenumbers, and another transmission window appears in the 23000-24000 cm^{-1}
262 range (violet domain). These spectra show two intense bands near 15500cm^{-1} and 17900 cm^{-1} (**Fig. 4**) that
263 correspond to the $^3T_1(F) \rightarrow {}^3T_1(P)$ transition of $^{[4]}Ni^{2+}$, split by the distortion of the $^{[4]}Ni^{2+}$ site (Jahn Teller
264 effect). The band near 22000 cm^{-1} due to $^{[5]}Ni^{2+}$, shows a dramatic decrease (in KB31 vs. KB27), in relation with
265 the disappearance of this coordination in KB35. The two bands located near 4800 and 8700 cm^{-1} are redshifted
266 and more intense than in the other borate glasses. The tetrahedral coordination of Ni^{2+} is confirmed by the
267 presence of the weak field-independent spin-forbidden transitions, $^3T_1(F) \rightarrow {}^1T_2(D)$ and $^3T_1(F) \rightarrow {}^1E(D)$ at
268 13000 cm^{-1} and 13900cm^{-1}, respectively [15].

269 The spectra of Na-borate glasses are depicted on **Fig.4b**. Though presenting a similar spectral shape and
270 position of the Gaussian components as in the LiB10, NaB10 and KB10 glasses (**Fig. A1**), the NaB20 glass
271 shows an absorption coefficient twice larger, as well as a modification of the absorption features in the near
272 infrared domain. This indicates the contribution of a new, non-resolved, Ni^{2+} speciation. The same trend towards
273 lower wavenumbers is observed in LiB30 and NaB30 glasses, with the main band shifted from 24000 to 22700
274 cm^{-1}. The most intense absorption band peaks outside the values usually found for $^{[6]}Ni^{2+}$. This characterizes the

formation of $^{[5]}Ni^{2+}$ sites. Together with the appearance of a contribution at 20000 cm^{-1} (on the low wavenumber side of the main absorption band), this shift causes the transmission window to shift from 17500 to 15000 cm^{-1}. Consequently, the color turns to yellow/brown hues. In the spectrum of NaB30, the absorbance at the position of the dashed vertical line indicates the appearance of minority tetrahedral Ni^{2+}. For Li-borate glasses **(Fig.4c)** there is also a red shift of the transitions with increasing alkali content, indicating a transformation from $^{[6]}Ni^{2+}$ to $^{[5]}Ni^{2+}$. By contrast to Na-borate glasses, the spectra do not show any contribution of tetrahedral Ni^{2+} even at high Li-content: the position of the dashed line corresponding to this coordination state falls in a transmission window. The spectrum of LiB30 may then be considered as typical of $^{[5]}Ni^{2+}$ and is described in more detail in 4.4.

4. Discussion

4.1 The speciation of Ni^{2+} in alkali borate glasses

4.1.1. Chemical dependence of the XANES features

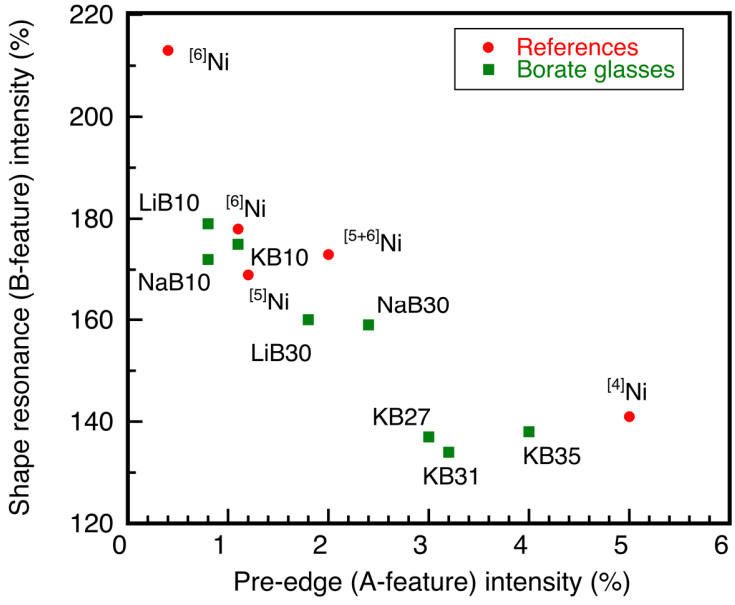

Fig. 5. Evolution of the intensity of the pre-edge (A feature) and of the main edge (B feature) for the XANES spectra of crystalline references and alkali borate glasses (see Fig. 1 and Fig. 2).

As for the crystalline references, the intensity of the two features A and B shows an opposite behavior as a function of the Ni-site geometry (**Fig. 5**). The relative intensity of the pre-edge varies by a factor 5 with Ni-coordination. The pre-edge and shape resonance intensity of $^{[5]}Ni^{2+}$ is intermediate between $^{[6]}Ni^{2+}$ and $^{[4]}Ni^{2+}$. In octahedral symmetry, as in $NiSO_4$, $6H_2O$, the pre-edge shows the lowest intensity. This intensity increases from $^{[5]}$- to $^{[4]}Ni^{2+}$ due to the hybridization of the Ni^{2+} *3d* and *4p* orbitals in non-centrosymmetric sites. Such hybridization explains also the decreasing intensity of the main edge, as it arises from transitions to *4p*-type levels. As depicted in **Fig. 5**, the XANES parameters of low alkali borate glasses correspond to what is expected for octahedral Ni^{2+}, as those of the K-rich KB31 and KB35 glasses correspond to majority tetrahedral Ni^{2+}. The XANES parameters of NaB30 and LiB30 glasses remain at values intermediate between $^{[6]}Ni^{2+}$ and $^{[4]}Ni^{2+}$, consistent with the presence of $^{[5]}Ni^{2+}$.

4.1.2. Discussion of the EXAFS-derived average coordination number of Ni^{2+}

Previous EXAFS data on alkali borate glasses have shown the presence of Ni^{2+} in 5- and 6-fold coordination in sodium borate glasses [24] and of 4-, 5- and 6 coordinated Ni^{2+} in lithium, sodium and potassium borate glasses (in the same samples as those here investigated) [11]. Both studies provide a similar picture of Ni-O distances and Ni-coordination number **(Fig. 6a)**, depicting a decrease of the Ni-O distances with increasing alkali content. The EXAFS-derived Ni-O distances exclude the presence of "exotic" coordination sites mentioned in earlier studies [4, 25] and further discussed in 4.1.3.

The average Ni-O distance and Ni coordination number decrease with increasing alkali content. The LiB10, NaB10 and KB10 glasses exhibit the same Ni-O distance at 2.04-2.05Å. This distance is smaller than expected for a regular octahedral site, typically 2.08Å in NiO. However, a decrease of the Ni-O distance by 0.02-0.04Å has been observed in NiO thin films [26] and some crystalline Ni borates may show $^{[6]}$Ni-O distances as low as 2.05-2.06Å [27]. The EXAFS parameters are consistent with the disappearance of $^{[6]}Ni^{2+}$ in alkali-rich borate glasses, with Ni-O distances smaller in K-bearing glasses. This indicates a higher concentration of tetrahedral nickel in K-borate glasses, as confirmed by the average Ni coordination number (**Fig. 6b**).

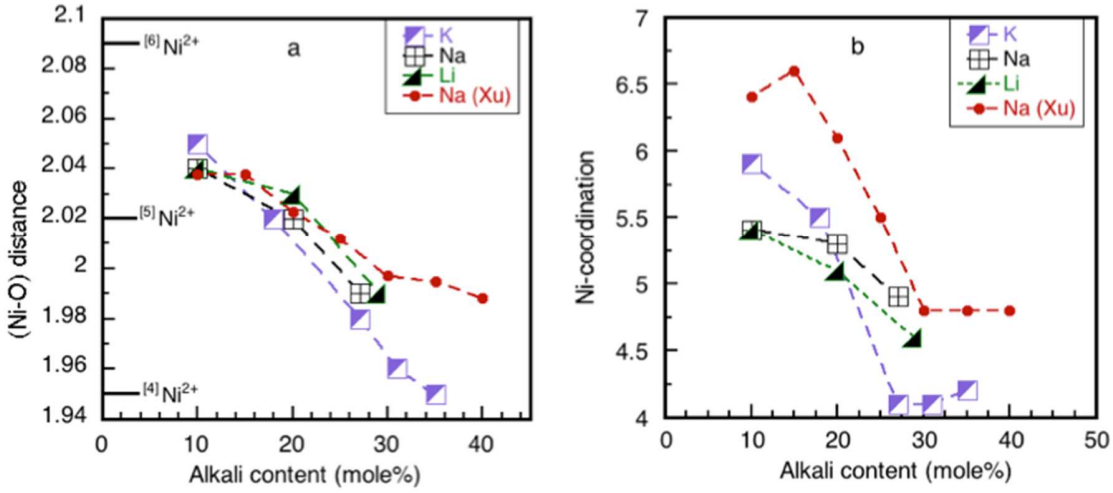

Fig. 6 Evolution of the EXAFS parameters of Ni^{2+} in alkali borate glasses from the data of [11] and [24]. Left: Ni-O distances; right: Ni-coordination number. The value of the Ni-O distances allows separate the contribution of 4-, 5- and 6-coordinated Ni.

4.1.3. Optical spectroscopic signatures of Ni^{2+}

Optical spectroscopic properties of Ni^{2+}-bearing borate glasses are characterized by a well-marked chemical dependence, interpreted as indicating a Ni coordination change with glass composition [3,4]. However, in the literature, Ni^{2+} coordination has been mostly determined from a qualitative discussion of crystal field spectra, interpreted as arising from $^{[6]}Ni^{2+}$ and $^{[4]}Ni^{2+}$. "Exotic" coordination numbers have also been evocated in the literature. The presence of 12-coordinated Ni^{2+} was mentioned in Na-borate glasses [25], despite such Ni^{2+} coordination is unknown [29]. Square-planar coordination or 8-coordinated Ni^{2+} were also evoked in alkali borate glasses [4, 28]. The optical properties of $^{[8]}Ni^{2+}$ in garnets [30] with optical transitions at 4000, 6000 and 20000 cm^{-1} characteristic of 8-coordinated Ni^{2+} do not correspond to the spectra observed in borate glasses. Moreover, EXAFS-derived Ni-O distances and XANES data, discussed in 3.1 for the square-planar coordination, exclude the presence of these unusual environments, which are packing-inefficient in oxide glasses.

The signature of three Ni^{2+} coordination states can be observed in the optical spectra of KB10, LiB30 and KB35 for $^{[6]}Ni^{2+}$, $^{[5]}Ni^{2+}$ and $^{[4]}Ni^{2+}$, respectively (**Fig. 7**). With increasing alkali content, the apparent maximum

of the main transition is redshifted, indicating a decreasing Ni^{2+} coordination (and hence decreasing crystal field intensity), as observed in crystalline references. As the optical transitions that characterize a Ni^{2+} coordination state do not vary much as a function of medium range surrounding [23], they can be used to determine Ni^{2+} coordination in glasses. This is especially true for the narrow $^{[4]}Ni^{2+}$ transition at 15600 cm^{-1}, identified by its small linewidth and located in a spectral domain, in which there is no optical transition caused by other Ni^{2+} speciations.

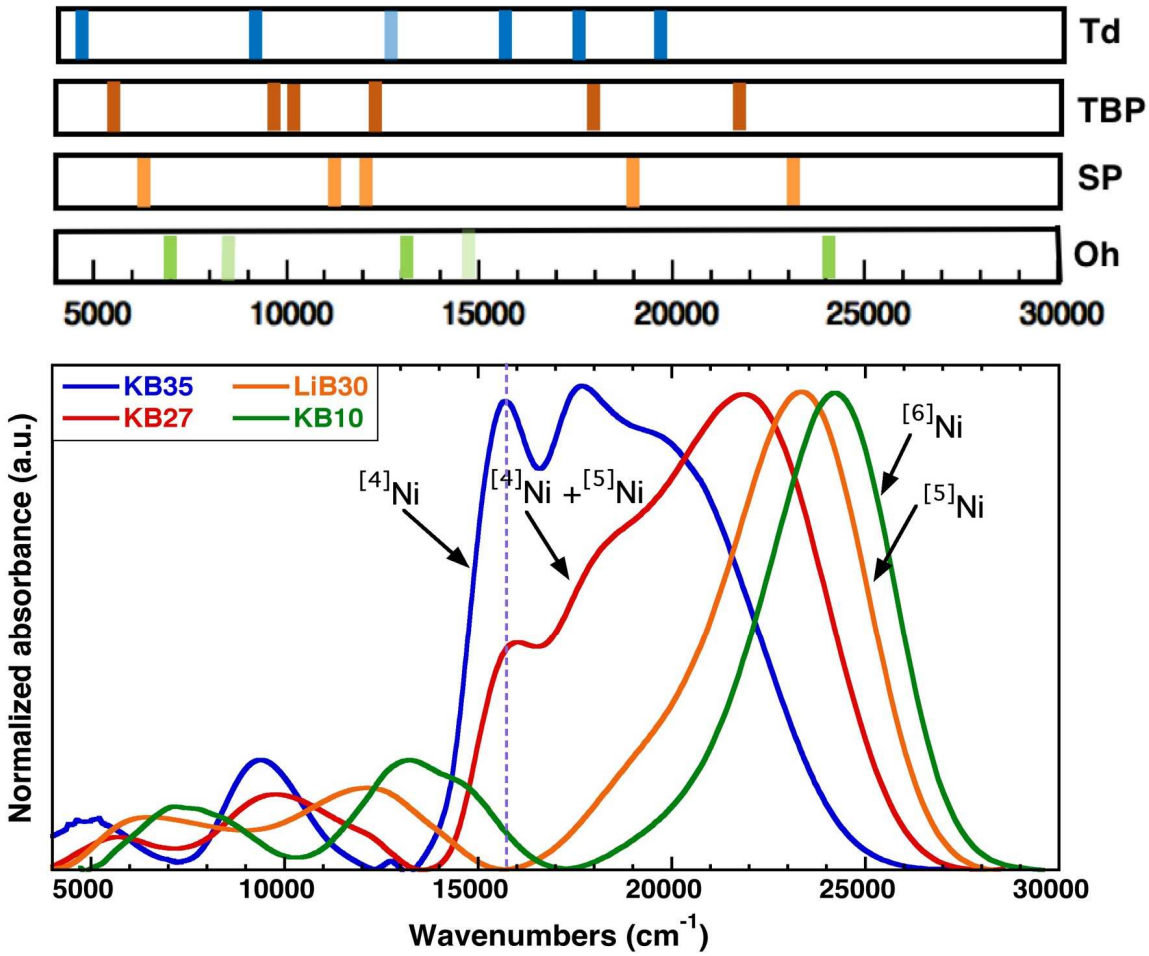

Fig. 7. Optical absorption spectra normalized to the most intense absorption band of each spectrum and corresponding to a dominant Ni^{2+} coordination. The top of the figure represents the optical transitions expected for the main coordination states. From top to bottom: $^{[4]}Ni^{2+}$, $^{[5]}Ni^{2+}$ in trigonal bipyramid (TBP) and in square pyramid geometry (SP) and $^{[6]}Ni^{2+}$.

4.1.4. Chemical dependence of Ni^{2+} coordination in alkali borate glasses.

The main absorption band occurs in the visible region at a position that depends on Ni^{2+} coordination. As this band is relatively sharp, its position determines the transmission window and hence the color of the glass. As shown on **Fig. 8a**, this band is redshifted from $^{[6]}Ni^{2+}$ to $^{[5]}Ni^{2+}$, defining a transmission window in the green and orange, respectively. In the case of $^{[4]}Ni^{2+}$ the intense characteristic transition near 15600 cm^{-1} causes a major change in the transmission window, which occurs on the high wavenumber side of this band, leading to a purple color.

The molar extinction coefficient ε of the most intense band is also chemically dependent, as it increases with increasing alkali content, with the largest variations observed for potassium glasses (**Fig. 8b**). Five coordinated and tetrahedral Ni^{2+} sites do not possess an inversion center and consequently display similar molar extinction coefficient (ε) values, which are higher than those of octahedral $^{[6]}Ni^{2+}$. This explains the limited increase of ε at high alkali content as already observed in Ni-bearing borate glasses [3,4]. As for the other spectroscopic parameters, ε values exhibit a continuous variation with glass composition, an additional evidence of the mixing of various coordination states of Ni^{2+} in alkali borate glasses.

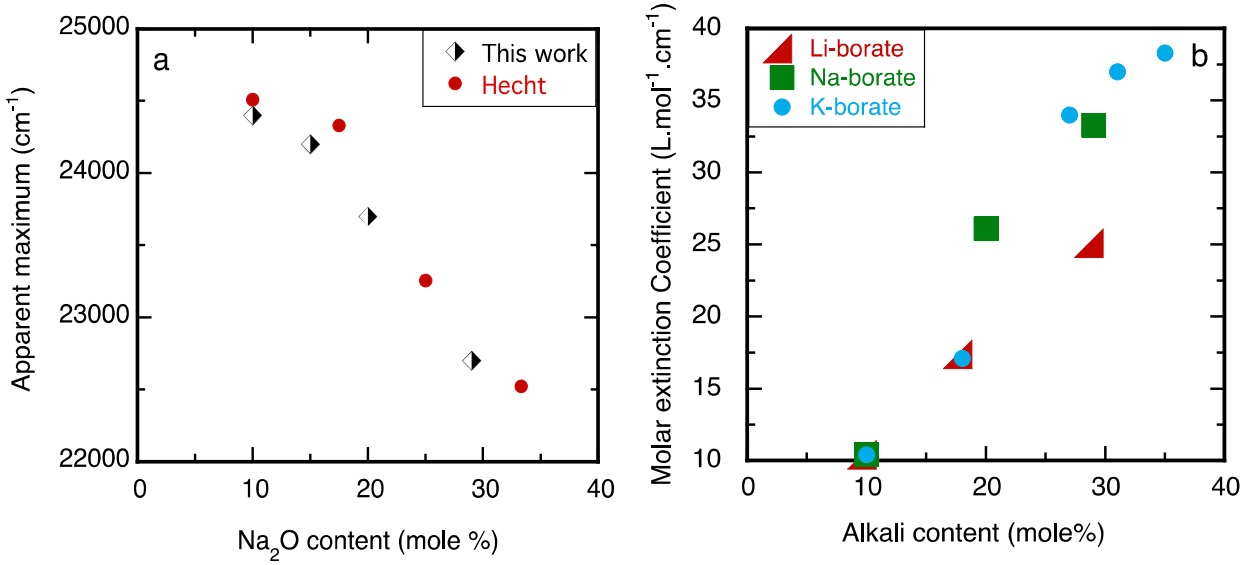

Fig. 8. a. Evolution of the apparent maximum of the most intense absorption band of Ni^{2+} in alkali borate glasses (in l/mol.cm). **b.** Evolution of the molar extinction coefficient ε with the alkali content.

368

369 *4.2. Structural significance of octahedral Ni^{2+}*

370

371 *4.2.1. Spectroscopic properties of octahedral Ni^{2+} in borate glasses.*

372 Although not observed in silicate and aluminosilicate glasses, 6-coordinated Ni is the prevailing
373 coordination state in low-alkali borate glasses, whatever the nature of the alkali. The optical absorption spectra
374 of low alkali borate glasses are the same for the three alkalis, indicating that crystal field splitting is not
375 influenced by the field strength of the alkali. The spectra can be fitted in six Gaussian components (**Fig. A1**).
376 The position of the absorption bands, with a crystal field splitting of 7500-8000 cm^{-1}, characterizes $^{[6]}Ni^{2+}$ [16,
377 23, 32]. However, the optical absorption bands (**Fig. A1**) cannot be fitted using a single Gaussian component
378 and the crystal field band shows a splitting of 1500 cm^{-1}, indicating a slight distortion of the Ni^{2+} site. These
379 spectra confirm the absence of NiO: NiO thin films show an absorption spectrum with the main bands at 28500,
380 21700 and 13500 cm^{-1} [33], these values being different from those observed in glasses near 24100, 13200 and
381 7500 cm^{-1}. This confirms the XANES results presented in 3.1.2.

382

383 *4.2.2. A peculiar property: the clustering of Ni^{2+} octahedra in low-alkali borate glasses.*

384 In low alkali glasses, alkali cations are consumed by the coordination change of boron: their charge-
385 compensating role for $^{[4]}B$ hinders their ability to play a similar role for Ni. This may explain the presence of 6-
386 coordinated Ni in ordered clusters [9-11], which do not require further charge compensation to be stabilized in
387 the glass structure. This behavior explains the independence of the spectroscopic properties of $^{[6]}Ni^{2+}$ on the
388 nature of the alkali for low-alkali borate glasses. These Ni-rich ordered domains have optical properties and a
389 local structure distinct from NiO [9,10]. Their formation may be related to the presence of rigid units such as
390 boroxol, pentaborate or tetraborate groups, which show only a limited coordination change of boron [1]. The
391 contribution of $^{[6]}Ni$ decreases with increasing alkali content as borate superstructural units are transformed into
392 smaller, less rigid units. This clustering is based on edge-sharing octahedra, an intersite linkage that is observed
393 in various nickel borates and Ni-substituted Mg borates, including ludwigite $Mg_2Ni(BO_3)O_2$, $Ni_2B_2O_5$
394 pyroborate, kotoite $Ni_3(BO_3)_2$ or $M^{2+}{}_2(M^{3+})(BO_3)O_2$ hulsite with two-dimensional Ni-domains [34]. In these

structures, divalent ions occur in distorted octahedra interlinked by edge-sharing and edge-linked to BO_3 units (**Fig. 9a**). These associations form 1D or 2D cationic domains, ribbons or ladders, such as in $Ni_2B_2O_5$ [35], though not as extended as the domains determined by EXAFS in low alkali (Li, Na, K) borate glasses [10].

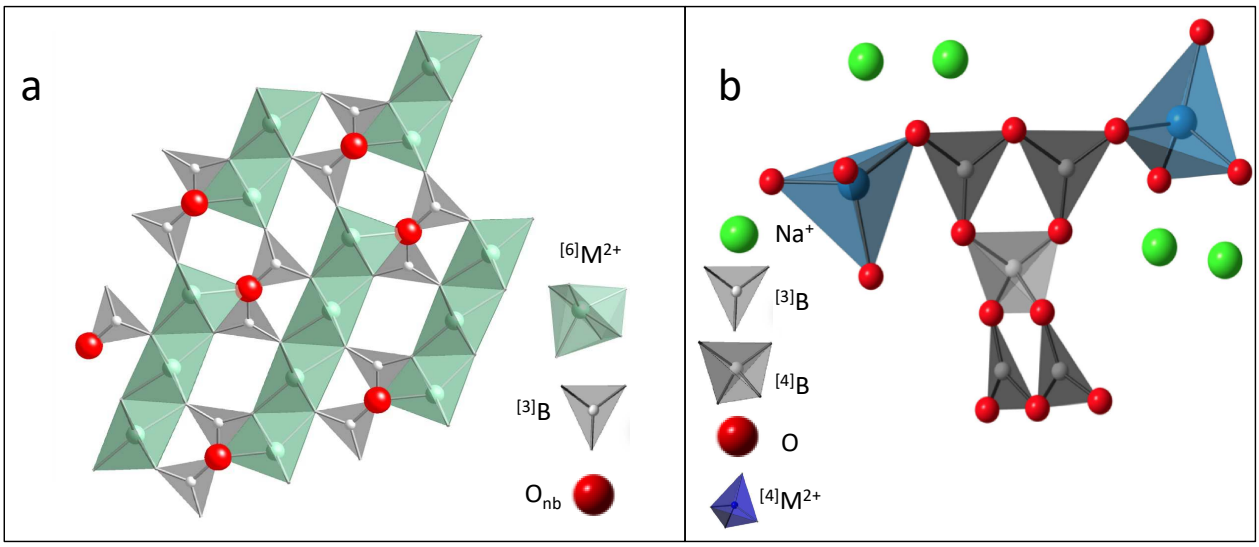

Fig. 9. a. Edge-sharing M^{2+}octahedra in the structure of $M_2B_2O_5$ pyroborate (after the data of [35]). Bridging oxygens bound to Ni are shown in red. Other oxygen atoms have been omitted. **b.** Tetrahedral M^{2+} in the structure of sodium transition-metal pentaborate $Na_3MB_5O_{10}$ showing a preferential association with $^{[3]}B$ (after [42], modified)

4.2.3. Links with physical properties of borate glasses

The presence of Ni-clustering may explain some properties of Ni-bearing low alkali (Li, Na, K) borate glasses: (i) the low solubility of NiO in these glasses at low alkali content [31] may be due to the difficulty of accommodating Ni-rich domains in the disordered structure of borate melts; this solubility increases with the alkali content, as these domains progressively disappear above 20 mol% alkali oxides [11]; (ii) the Ni^{2+} Electron Paramagnetic Resonance (EPR) signal vanishes below 200K in Na-borate glasses [13], indicating a transition at low temperature from a superparamagnetic to an (anti)ferromagnetic state, compatible with the presence of NiO-based clusters; such transition from a paramagnetic to an antiferromagnetic state at Neel temperature has also been observed by EPR in nano-NiO particles [36]; (iii) the magnetic moment increases with alkali

concentration [37], which has been interpreted as indicating a decreasing contribution of $^{[6]}Ni^{2+}$ up to an alkali concentration of about 20 mol%, above which Ni^{2+} occurs in lower coordinated sites.

4.3. Structural significance of tetrahedral Ni^{2+}

4.3.1. Spectroscopic properties of tetrahedral Ni^{2+} in borate glasses.

There is a major influence of the nature of the alkali on the proportion of $^{[4]}Ni^{2+}$, a coordination state which is not detected in Li-borate glasses and remains a minority in Na-borate glasses. The presence of $^{[4]}Ni^{2+}$ in K_2O-rich borate glasses has been observed since decades by optical spectroscopy [4]. The distortion of the $^{[4]}Ni^{2+}$ site, arising from a static Jahn-Teller effect, is shown by optical spectroscopy (see 3.2.2). The tetrahedral coordination of Ni^{2+} is confirmed by XANES (see 4.1.2) and by the EXAFS-derived $^{[4]}$Ni-O distances, around 1.95Å [15]. The low value of the EXAFS Debye-Waller factor found in these glasses [15] indicates that the site distortion detected by optical spectroscopy results from angular distortion of the Ni-site rather than a distribution of Ni-O distances. The spectroscopic properties of $^{[4]}Ni^{2+}$ are similar to those encountered in silicate and aluminosilicate glasses [15,21,38], showing that $^{[4]}Ni^{2+}$ sites in oxide glasses are independent on the type of glass. In silicate glasses, these sites are consistent with a network-former position, provided two alkali ions are present for charge compensation [15]. However, the small intensity of a Ni–B contribution prevents the direct detection by EXAFS of a linkage with the borate network, contrary to the Ni–Si contribution detected around $^{[4]}Ni^{2+}$ in silicate and aluminosilicate glasses [21,38].

The structure of borate crystals is of interest to suggest various geometries of the linkage between tetrahedral divalent cations (Zn^{2+}, Mg^{2+}…) and the borate framework. For instance, tetrahedral Zn is preferentially linked by corner-sharing with BO_3 triangles in $Na_3ZnB_5O_{10}$ [39] and $Li_{0.48}Na_{0.52}ZnBO_3$ [40]. Sodium pentaborates $Na_3MB_5O_{10}$ (M=Co, Fe^{2+}) also show a linkage of tetrahedral divalent cations with BO_3 triangles (**Fig. 9b**). High temperature favors also tetrahedral coordination of small divalent cations, as shown by the coordination of Zn^{2+} in the $LiZnBO_3$ polymorphs: as ZnO_4 tetrahedra exist in the high temperature phase, the low temperature polymorph shows trigonal bipyramidal Zn [41]. A preferential bonding to BO_3 triangles may be rationalized by considering bond valence constraints [14]: trigonal B brings a charge compensation of 1 for the

oxygen atoms, as compared to 0.75 for tetrahedral B, which minimizes the charge deficit of the oxygen involved in the bond to a tetrahedral cation.

4.3.2. Links with physical properties of borate glasses.

The presence of $^{[4]}Ni^{2+}$ sites requires the charge deficit be compensated by alkalis. This means a competition with boron for charge compensation, as was observed in Zr alumino-borosilicates where it was possible to determine the relative preference for charge compensation between various cations [43]. This competition may explain the chemical dependence of the proportion of $^{[4]}Ni^{2+}$ observed in some K- and Na-borate glasses (there is no measurable $^{[4]}Ni^{2+}$ in Li-borate glasses and in alkali-poor borate glasses compositions). By contrast to borate glasses, the $^{[4]}Ni^{2+}$ proportion remains almost independent on alkali concentration in silicate glasses [8,44]. The competition for charge compensation may be responsible for the decrease of Ni-solubility above about 30 mol% alkalis in borate glasses, as the formation of stable borate superunits will require alkalis to stabilize the $^{[4]}B$ sites they contain instead of Ni-sites. Finally, an increasing proportion of $^{[4]}Ni^{2+}$ at increasing alkali content may explain the continuous increase of the magnetic moment [37].

4.4. Structural significance of five-coordinated Ni^{2+}

Several optical absorption spectra of $^{[5]}Ni^{2+}$ in crystalline borates, phosphates and silicates have been published recently because of the interest for environmentally-friendly brown pigments: $LiMgBO_3$:Ni [45], NiB_4O_7 [46], $Ni_2P_2O_7$ (8,47), $SrNiP_2O_7$ [20], $KNiPO_4$ [8,48] or $BaZn_{2-x}Ni_xSi_2O_7$ and $BaMg_{2-x}Ni_xSi_2O_7$ sorosilicates [49]. The local structure of $^{[5]}Ni^{2+}$ in two borate crystals is depicted on **Fig. 10**, showing that this coordination state may be associated to either triangular or tetrahedral borate groups.

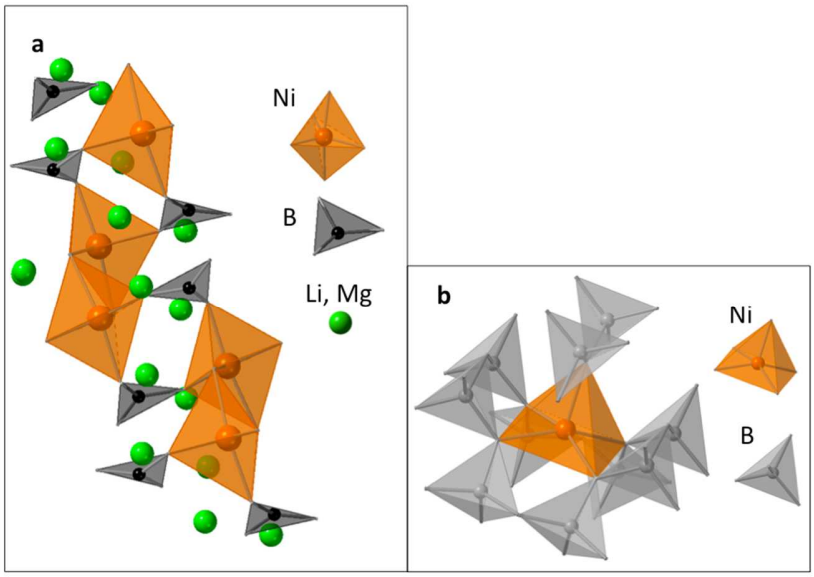

Fig. 10. The two main geometries of five-coordinated Ni: **a.** trigonal bipyramid in $LiMgBO_3$:Ni^{2+} (after the data of [45], modified) with linkages to triangular B units; **b.** square pyramid in ß-NiB_4O_7 (after the data from [46], modified), with linkages to tetrahedral B units.

The presence of $^{[5]}Ni^{2+}$ in borate glasses at medium Na- and K content and medium to high Li content is shown by three kinds of spectroscopic evidences, which are exemplified in the LiB30 glass. (i) The XANES features such as pre-edge and shape resonance intensity are intermediate between those of $^{[4]}$- and $^{[6]}$Ni. (ii) Similarly, EXAFS data indicate a mixture of $^{[4]}Ni^{2+}$ and$^{[5]}Ni^{2+}$ at medium Na- and K-concentrations, with EXAFS-derived Ni-O mean distances of about 1.98Å and a Ni mean coordination number around 5. (iii) Crystal field spectra are similar to those first described in brown Ni-bearing silicate and aluminosilicate glasses [8,38]. These spectra may be fitted with 6 Gaussian components (**Fig. A2**), which are located at energy positions characteristic of $^{[5]}Ni^{2+}$ (**Fig. 11a and b**). The main band near 23400 cm^{-1} shows a Gaussian shape on its high wavenumber side, an indication of the absence of $^{[6]}Ni^{2+}$ expected at or above 25000 cm^{-1}.

Decreasing crystal field intensity arises from a number of ligands smaller in 5-coordination relative to an octahedral site. However, the shorter Ni–O distances in 5- vs. 6-coordination may partly compensate lower crystal field splitting values. The result is a red shift of about 1000-2000 cm^{-1} of the $^{[5]}Ni^{2+}$ optical transitions relative to those of $^{[6]}Ni^{2+}$ (**Fig. 11b**). This shift can be considered as a spectroscopic signature of 5-coordinated

480 Ni^{2+}. The most intense band at 23400 cm^{-1} and the shoulder near 20000 cm^{-1} correspond to transitions to ^3P
481 levels, the position of which depends on covalence effects. Their position is intermediate between that measured
482 in spectra of $^{[4]}Ni^{2+}$ and $^{[6]}Ni^{2+}$, a nice illustration of the intermediate covalence of $^{[5]}Ni^{2+}$-O bonds (**Fig. 7**).
483

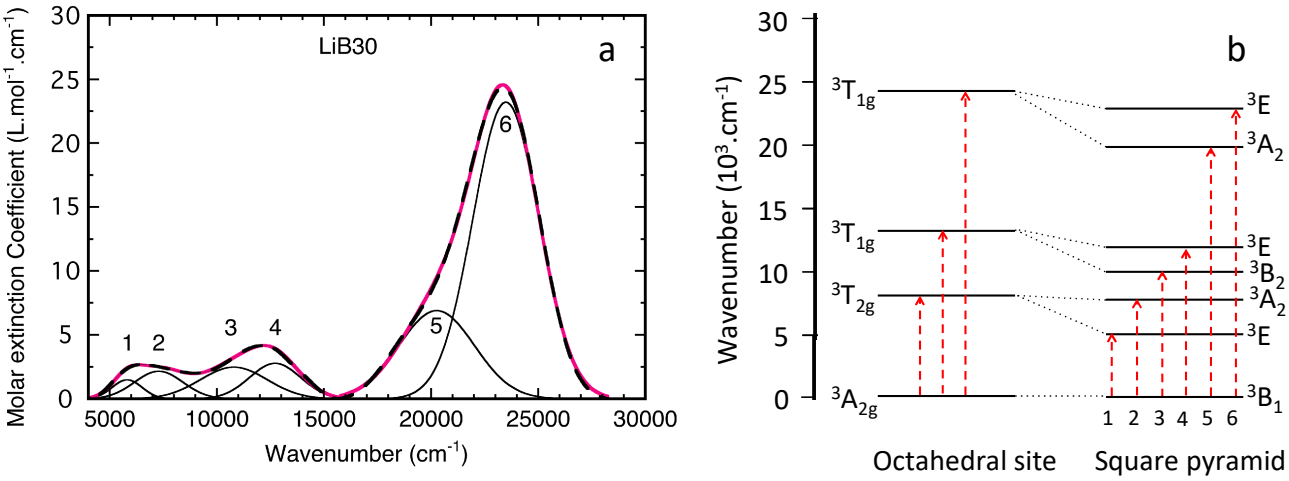

484
485 **Fig. 11. a.** Gaussian fit of the optical absorption spectrum of LiB30 glass corresponding to $^{[5]}Ni^{2+}$ in a square
486 pyramid geometry. **b.** Energy levels of $^{[6]}Ni^{2+}$ in regular octahedral coordination and $^{[5]}Ni^{2+}$, showing the redshift
487 of the main optical transitions from octahedral to square pyramid geometry. The assignments are based on [50].
488
489 *4.5. The driving mechanism of* Ni^{2+} *coordination change in borate glasses*

490 The coordination number of a cation is correlated with the field strength of the other cations. If these
491 cations have a higher field strength, defined as the ratio of the net charge Z and the square of the average bond
492 distance to oxygen d (Z/d^2), they will take more of the electron density from the O atoms and they will have a
493 higher acidic character. A larger Ni coordination number is then required to balance the Ni^{2+} charge. The
494 investigation of a large number of Ni-bearing alkali silicate and aluminosilicate glasses [8,38] shows that Ni^{2+}
495 coordination changes as a function of cation field strength, low field strength K^+ stabilizing $^{[4]}Ni^{2+}$ as higher
496 field strength Na^+ rather stabilizes $^{[5]}Ni^{2+}$.

497 Octahedral coordination of Ni^{2+} is observed in alkali-poor borate glasses, the structure of which is
498 dominated by superstructural units [1]. In these glasses, the addition of alkalis favors BO_4 tetrahedral structural
499 units, rather than the formation of nonbridging oxygen atoms (NBO). The 6-fold coordination state of Ni^{2+}, may

500 arise from a competition for available ligands, due to the strength of the B-O bonds relative to the weaker Ni-O
501 bonds [3]. In intermediate, more basic compositions, for which not all the ligands are strongly bound to other
502 cations, the optical spectra indicate a band at greater wavenumbers than that of $^{[4]}Ni^{2+}$. The present work assigns
503 this band to a signature of $^{[5]}Ni^{2+}$, on the basis of optical absorption, XANES and EXAFS spectra. Finally, in the
504 most alkali-rich glasses, which show the highest concentration of $^{[4]}B$, the bond valence model predicts that the
505 connection of $^{[4]}Ni^{2+}$ to a bridging oxygen between two B tetrahedra satisfies the charge deficit of this bridging
506 oxygen. The predominance of $^{[4]}Ni^{2+}$ in high K-borate glasses shows that the remaining deficit of this tetrahedral
507 divalent cation can only be ensured by low field strength cations. These cations also stabilize $^{[4]}Ni^{2+}$ in silicate
508 and aluminosilicate glasses [3,4,8,38,44].
509 $^{[5]}Ni^{2+}$ may be seen as a reactive intermediate in reactions involving ligand exchange, such as those
510 operating during viscous flow (**Fig. 12**). This would be equivalent to the presence of a minority five-coordinated
511 Al or Si species in silicate and aluminosilicate glasses, corresponding to local bond-breaking and rearrangement
512 that characterizes the dynamics of the molten state [51]. At the difference of the directional, covalent B-O
513 bonds, the weaker Ni-O bonds are more prone to be broken because of their ionic and hence non-directional
514 nature, inducing that Ni^{2+} is mostly found in 5-fold coordination. Even if Ni^{2+} has the highest crystal field
515 stabilization energy (CFSE) in 6-fold coordination, the relative concentration of these transition states is thus
516 expected to be more important than for network former cations that are only marginally affected by this
517 transient coordination change. It is interesting that, in hydrothermal solutions, experimental data and first
518 principles calculations show also the presence of 5-coordinated Ni^{2+} forming $^{[5]}Ni^{2+}$-triborate complexes [52].
519
520

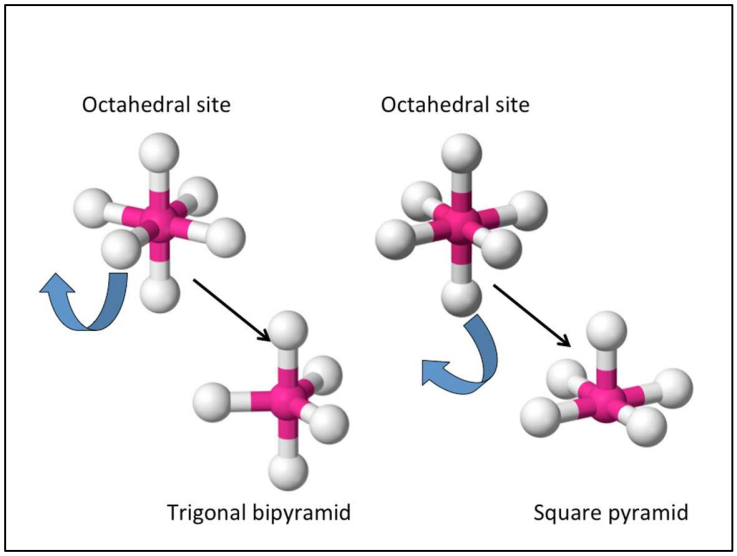

Fig. 12. Generation of a 5-coordinated site, trigonal bipyramid (left) or square pyramid (right) during atomic motion and bond breaking associated to the viscous flow of a melt.

Crystal field stabilization energy (CFSE) considerations also favor the abundance of $^{[5]}Ni^{2+}$. CFSE is $12Dq$ and $10Dq$ for $^{[6]}Ni^{2+}$and $^{[5]}Ni^{2+}$, respectively, Dq being the crystal field splitting parameter. The smaller number of ligands results in smaller Dq values for $^{[5]}Ni^{2+}$ relative to $^{[6]}Ni^{2+}$. However, $^{[5]}Ni^{2+}$-O distances are smaller than $^{[6]}Ni^{2+}$-O distances, which increases CFSE values. Finally, the difference between the CFSE of $^{[6]}$- and $^{[5]}Ni^{2+}$, remains small, about 1.5 kJ.mole^{-1} [21]. This explains the potential stability of 5-coordinated Ni^{2+} in oxide glasses.

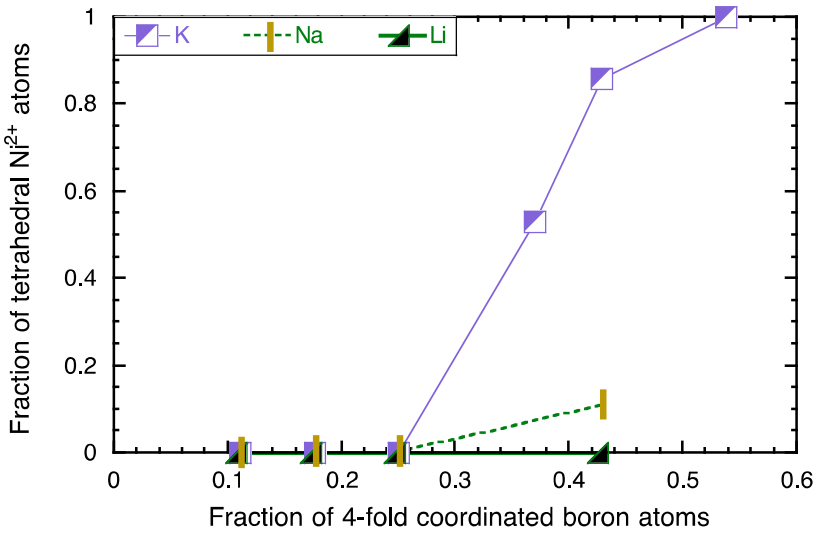

Fig. 13. Chemical dependence of Ni coordination in alkali borate glasses. The $^{[4]}Ni^{2+}$fraction is derived from the intensity of the $^{[4]}Ni^{2+}$absorption band near 17000 cm^{-1}.

An estimate of the relative proportion of $^{[4]}Ni^{2+}$and $^{[5]}Ni^{2+}$ can be derived from the intensity of the 17000 cm^{-1} absorption band of $^{[4]}Ni^{2+}$, under the assumption that the molar absorption coefficient ε of $^{[4]}Ni^{2+}$remains constant among the glasses. The chemical dependence may be quantified through the average B-coordination, defined by the N_4 parameter: $N_4 = {}^{[4]}B/({}^{[3]}B+{}^{[4]}B)$. It has been shown that the N_4 value corresponds to the molar ratio of alkali to boron [53]. The proportion of $^{[4]}Ni^{2+}$ranges between almost 100% to less than a few %, in the K-rich and alkali poor borate glasses, respectively (**Fig. 13)**

At higher network-modifier fractions, the depolymerization of the borate network favors the formation of NBO's. In the presence of Ni^{2+}, alkalis play a dual role in charge compensating $^{[4]}Ni^{2+}$and interacting with the borate network. The relatively large field strength of lithium favors the formation of $^{[4]}B$ [54], which explains the absence of $^{[4]}Ni^{2+}$ units. By contrast, larger alkalis generate higher proportions of NBO's because their lower field strength, which explains that alkalis may be involved in charge compensating $^{[4]}Ni^{2+}$units. **Figure 13** demonstrates that there is no direct relation between the chemical dependence of Ni and B coordination numbers: the structure of the polymeric network does not provide an objective estimate of Ni^{2+} speciation.

As pointed out by Adrian Wright [1], the network-modifying cations play a critical role in the structure of borate glasses, although this role is frequently overlooked. The high temperature data of Lin and Angell [55]

552 provide an enlightening illustration of this behavior, demonstrating that $^{[4]}Ni^{2+}$ concentration in borate glasses
553 and melts increases from the glassy to the molten state. This variation is related to a modification of the role of
554 alkalis associated to the coordination change of boron during the melting of borate glasses [56], according to the
555 relation describing the change of the role of the alkali M:

556 $$BO_4 + M_{comp} \rightarrow BO_3 + O_{nb} + M_{mod}$$

557 where M_{comp} and M_{mod} refer to a charge-compensating or modifying role of the alkali and O_{nb} designates a non-
558 bridging oxygen. This means that alkali "activity" increases in the melt, making them available for charge-
559 compensating $^{[4]}Ni^{2+}$.
560
561 *4.6. Comparison with the role of Mg^{2+} in borate glasses*
562 Divalent nickel often mimics the structural behavior of Mg^{2+} due to the similarity in their ionic radius. In
563 alkali silicate and aluminosilicate glasses and melts, Mg^{2+} is present in 4-, 5- and minority 6-fold coordination,
564 the relative proportion of which follows a similar dependence as Ni^{2+} as a function of glass composition [57,
565 58]. The investigation of Mg coordination in Na-Mg borate glasses [59] and K-Mg borate glasses [60] has
566 shown the presence of $^{[6]}Mg$ or $^{[4]}Mg$ in alkali-poor and alkali-rich compositions, respectively. This observation
567 is in line with the present results deduced from the spectroscopic properties of Ni in these glasses. In alkaline
568 earth borate glasses, the proportion of tetrahedral boron, N_4, increases with the concentration of alkalis and
569 alkaline earths [61]. However, the N_4 value decreases from Ba to Mg. This dependence on the cation field
570 strength is reverse to what is observed in alkali borate glasses [62]. This observation is consistent with the
571 structure of crystalline Mg-borates, showing a preferential association of Mg sites with triangular borate units.
572 As discussed above, this structural property is expected from the bond valence model and may drive the local
573 structure around Mg in borate glasses.
574 Finally, a recent study on borosilicate glasses [63] demonstrated that the most salient structural effect of
575 the incorporation of Mg is an increase in the $^{[3]}B$ population. This effect can be attributed to the larger cation
576 field strength of Mg^{2+} relative to that of other network-modifying cations. This was ascribed to the poor
577 capability of Mg^{2+} for charge-compensating the charge deficit of $^{[4]}B$ units due to relatively high field strength.
578 The local structure around Ni is then similar to that of Mg, with a specific linkage of $^{[4]}Ni^{2+}$ with triangular $^{[3]}B$

579 units. Such association may help in rationalizing the structure of borate glasses, as the building blocks used to
580 describe the topology of crystalline borates [64] may give some insight on the local structure of borate glasses.
581
582 **5. Conclusion**
583 A detailed picture of the speciation of Ni^{2+} in alkali borate glasses was obtained by coupling optical
584 absorption spectroscopy with Ni K-edge XANES and previous EXAFS data. These glasses show a broad range
585 of colors of as a function of alkali field strength, from yellow and brown to purple. The absorptivity of
586 tetrahedral and five-coordinated Ni^{2+} is similar, a property that gives all intermediate alkalinity borate glasses
587 the same brown color as silicate and aluminosilicate glasses containing an alkali with the same field strength.
588 Our results update previous descriptions of the optical spectra of Ni^{2+} in alkali borate glasses based on the
589 coexistence of only octahedral and tetrahedral Ni^{2+}. By using complementary spectroscopic methods, we show
590 that nickel speciation in borate glasses corresponds to the coexistence of $^{[4]}$-, $^{[5]}$- and $^{[6]}Ni^{2+}$, each coordination
591 state having a specific structural position: clusters of $^{[6]}$Ni edge-sharing octahedra at low alkali content, $^{[4]}$Ni
592 tetrahedra connected to the borate network in presence of low field strength elements as charge compensators
593 and $^{[5]}$Ni sites corresponding to reactive species that inherit from molten state dynamics in presence of medium
594 field strength elements. Cation field strength defines the capacity of alkalis to charge compensate $^{[4]}$B and
595 $^{[4]}Ni^{2+}$, and plays a crucial role in controlling the local structure around Ni^{2+} in these glasses. This causes $^{[4]}Ni^{2+}$
596 to be stabilized in high K-borate glasses. The quantification of the proportion of tetrahedral Ni^{2+} shows a non-
597 linear dependence on alkali concentration. This results from a competition for charge compensation between Ni
598 and B, as already observed in other glasses. The inefficiency of Li to charge compensate $^{[4]}Ni^{2+}$ explains the
599 absence of this coordination in Li-borate glasses. Due to the many similarities between Ni^{2+} and Mg^{2+}, the
600 diversity of the structural scenarios around Ni^{2+} in alkali borate glasses may shed light on the structural behavior
601 of Mg in the same glasses, underlining the diversity of local structures around these divalent cations, as a
602 function of glass composition.
603
604
605

Acknowledgements

We gratefully acknowledge the support of Institut Universitaire de France. We also thank Franck Hawthorne for sharing his knowledge on the structural logic of borate minerals.

Appendix:

Gaussian fits of the investigated glasses

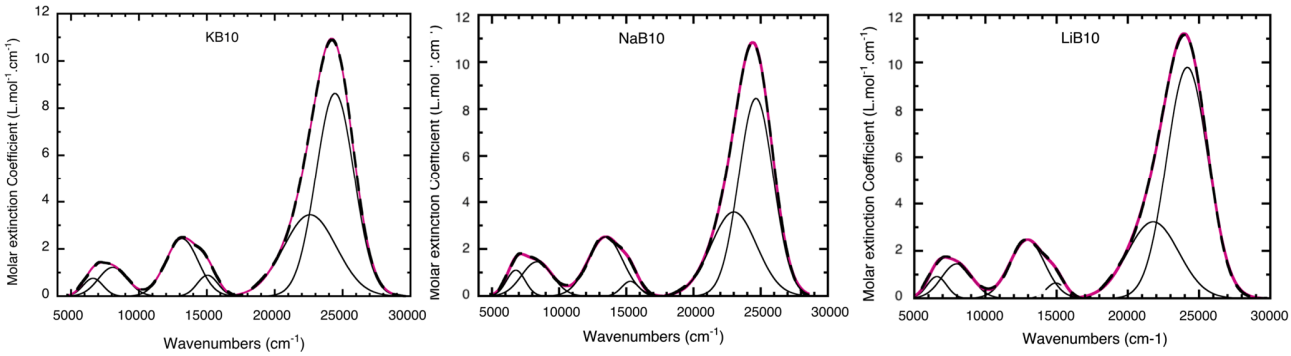

Figure A1. Optical absorption spectra of Ni^{2+} in 10 mol% alkali borate glasses: the optical spectra have the same shape and can be fitted with the same components. The transitions are those expected from the energy level diagram of Figure 11b. The fit shows that the three main bands are splitted, due to a slight site distortion.

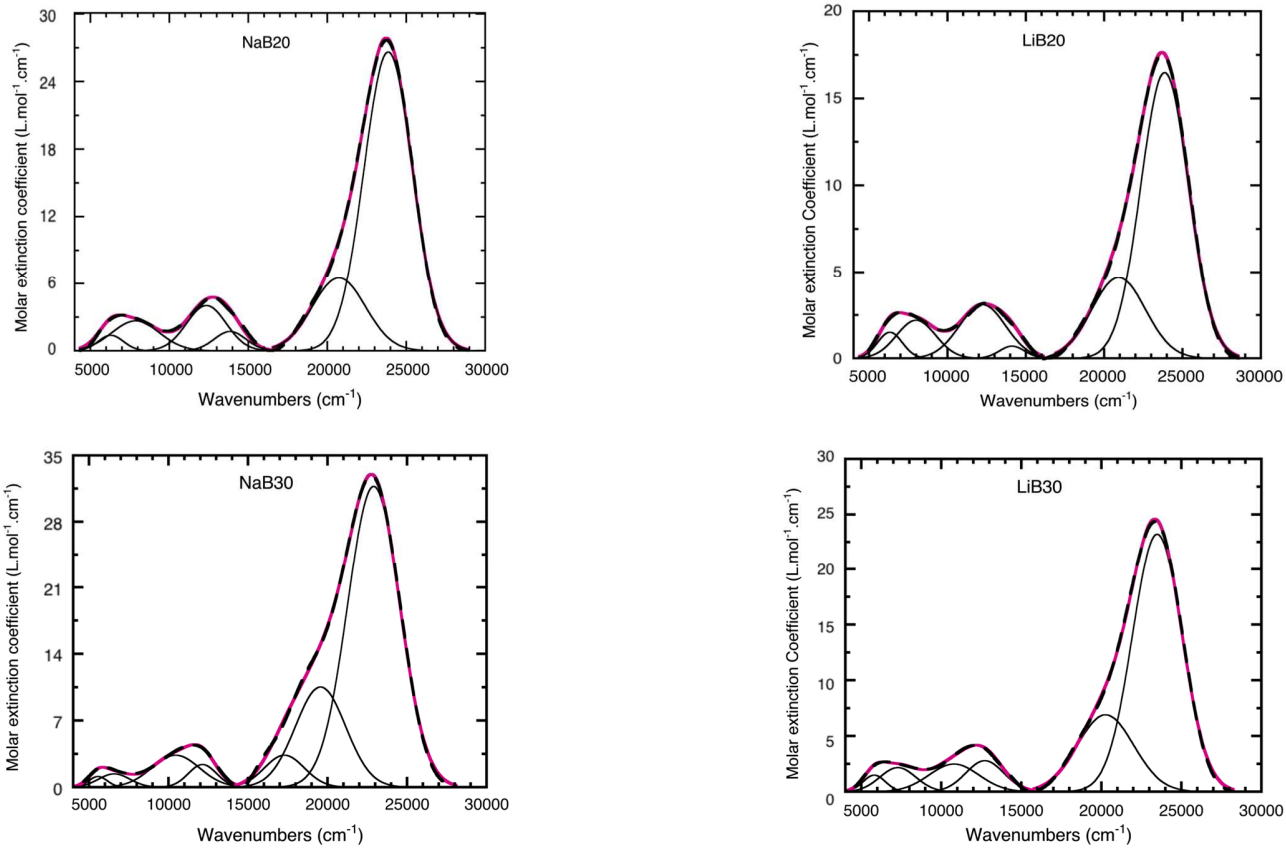

Figure A2. Optical absorption spectra of Ni^{2+} in 20 and 30 mol% alkali borate glasses: the spectra of NaB20 and LiB20 are similar to those of 10 mol% alkali, with an increasing non-Gaussian character of the components in the near IR region, showing a higher distortion of the $^{[6]}Ni^{2+}$ site. The optical spectrum of NaB30 shows the appearance of tetrahedral Ni^{2+} with a characteristic transition near 17000 cm^{-1}. The spectrum of LiB30 is typical for 5-coordinated Ni (see **Fig. 11a and b**).

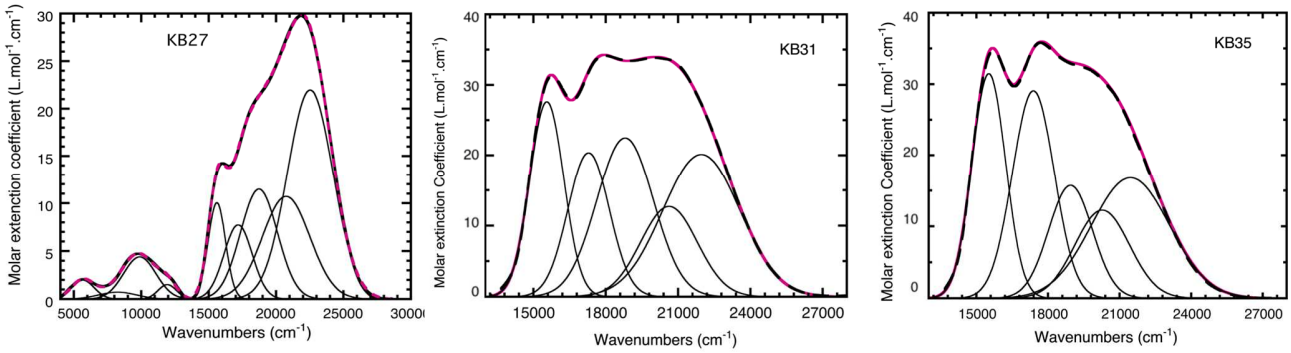

Figure A3. Optical absorption spectra of Ni^{2+} in high K borate glasses. With increasing K-content, the

628 contributions near 16000 and 18000 cm^{-1} related to tetrahedral Ni^{2+} increase . The intense component near 23000
629 cm^{-1} corresponds to the main contribution of $^{[5]}Ni^{2+}$ in the KB27 glass. It progressively decreases at higher K-
630 content.
631
632 **REFERENCES**

633 [1] A.C. Wright, My borate life: an enigmatic journey, Int. J. Appl. Glass Sci. 6 (2015) 45-63.
634 DOI:10.1111/ijag.12113
635 [2] W.A. Weyl, Coloured Glasses, Society of Glass Technology, 1951.
636 [3] J. Wong, C.A. Angell, Glass structure by spectroscopy, M. Dekker, New York, 1976.
637 [4] A. Paul, R.W. Douglas, Co-ordination equilibria of nickel (II) in alkali borate glasses, Phys. Chem.
638 Glasses. 8 (1967) 233–237.
639 [5] L. Galoisy, G. Calas, L. Cormier, B. Marcq, M.H. Thibault, Overview of the environment of Ni in oxide
640 glasses in relation to the glass colouration, Phys. Chem. Glasses. 46 (2005) 394–399.
641 [6] M.O.J.Y. Hunault, L. Galoisy, G. Lelong, M. Newville, G. Calas, Effect of cation field strength on Co2+
642 speciation in alkali-borate glasses, J. Non-Cryst. Solids 451 (2016) 101–110.
643 DOI:10.1016/j.jnoncrysol.2016.06.025
644 [7] M.O.J.Y. Hunault, G. Lelong, L. Cormier, L. Galoisy, P.L. Solari, G. Calas, Speciation change of uranyl
645 in lithium borate glasses, Inorg. Chem. 58 (2019) 6858-6865. DOI: 10.1021/acs.inorgchem.9b00305
646 [8] L. Galoisy, G. Calas, Structural environment of nickel in silicate glass/melt systems. I. Spectroscopic
647 determination of coordination states, Geochim. Cosmochim. Acta 57 (1993) 3613–3626. DOI:10.1016/0016-
648 7037(93)90143-K
649 [9] L. Cormier, L. Galoisy, G. Calas, Evidence of Ni-containing ordered domains in low alkali borate
650 glasses, Europhys. Lett. 45 (1999) 572-578. DOI:10.1209/epl/i1999-00205-7
651 [10] L. Galoisy, L. Cormier, G. Calas, V. Briois, Environment of Ni, Co and Zn in low alkali borate glasses:
652 information from EXAFS and XANES spectra, J. Non-Cryst. Solids 293-295 (2001) 105-111.
653 DOI:10.1016/S0022-3093(01)00659-7

[11] L. Galoisy, G. Calas, L. Cormier, Chemical stability of Ni-enriched nanodomains in alkali borate glasses, J. Non-Cryst. Solids 321 (2003) 197-203. DOI: 10.1016/S0022-3093(03)00232-1

[12] A. Terczyńska-Madej, K. Cholewa-Kowalska, M. Łączka, Coordination and valence state of transition metal ions in alkali-borate glasses, Opt. Mater. 33 (2011) 1984-1988. DOI: 10.1016/j.optmat.2011.03.046

[13] H.G. Hecht, Study of the structure of nickel in soda-boric oxide glasses, J. Chem. Phys. 47 (1967) 1840-1843. DOI: 10.1063/1.1712177

[14] L. Galoisy, G. Calas, Spectroscopic evidence for five-coordinated Ni in $CaNiSi_2O_6$ glass, Amer. Miner. 76 (1991) 1779 – 1782.

[15] L. Galoisy, G. Calas, Network forming nickel in silicate glasses. Amer. Miner. 77 (1992) 677-680.

[16] A. Manceau, G. Calas, A. Decarreau, Nickel-bearing clay minerals: 1. Optical spectroscopic study of nickel crystal chemistry, Clay Miner. 20 (1985) 367-387. DOI: 10.1180/claymin.1985.020.3.08.

[17] T.D. Keene, D. Rankine, J.D. Evans, P.D. Southon, C.J. Kepert, J.B. Aitken, C.J. Sumby, C.J. Doonan, Solvent-modified dynamic porosity in chiral 3D kagome frameworks, Dalton T. 42 (2013) 7871-7879. DOI: 10.1039/C3DT00096F.

[18] G.E. Brown Jr, G. Calas, G.A. Waychunas, J. Petiau, X-ray absorption spectroscopy and its applications in mineralogy and geochemistry, Rev. Mineral. 18 (1988) 431-512. DOI: 10.1515/9781501508974-013

[19] C. Gougoussis, M. Calandra, A. Seitsonen, C. Brouder, A. Shukla, F. Mauri, Intrinsic charge transfer gap in NiO from Ni K-edge x-ray absorption spectroscopy, Phys. Rev. B79 (2009) 045118. DOI: 10.1103/PhysRevB.79.045118.

[20] A. El Jazouli, B. Tbib, A. Demourgues, M. Gaudon, Structure and colour of diphosphate pigments with square pyramid environment around chromophore ions (Co^{2+}, Ni^{2+}, Cu^{2+}), Dyes Pigm. 104 (2014) 67–74. DOI: 10.1016/j.dyepig.2013.11.021

[21] L. Galoisy, G. Calas, Structural environment of nickel in silicate glass/melt systems. II. Geochemical implications, Geochim. Cosmochim. Acta 57 (1993) 3627–3633. DOI: 10.1016/0016-7037(93)90144-L

[22] M. Moutataouia, F. El Bachraoui, Y. Tamraoui, M. Lamire, S. Krimi, B. Manoun, Crystal structure and optical properties of a new nickel magnesium diphosphate, J. Mol. Struct. 1223 (2021) 128983. DOI: 10.1016/j.molstruc.2020.128983

[23] G.R. Rossman, R.D. Shannon, R.K. Waring, Origin of the yellow color of complex nickel oxides, J. Solid St. Chem. 39 (1981) 277-287. DOI: 10.1016/0022-4596(81)90261-9

[24] Q. Xu, T. Maekawa, K. Kawamura, T. Yokokawa, Local structure around Ni^{2+} ions in sodium borate glasses, Phys. Chem. Glasses 31 (1990) 151-155.

[25] J. S. Berkes, W.B. White, The optical spectra of nickel in alkali tetraborate glasses, Phys. Chem. Glasses 7 (1966) 191-199.

[26] A. Anspoks, A. Kalinko, R. Kalendarev, A. Kuzmin, Atomic structure relaxation in nanocrystalline NiO studied by EXAFS spectroscopy: role of nickel vacancies, Phys. Rev. B 86 (2012) 174114. DOI: 10.1103/PhysRevB.86.174114

[27] M.K. Schmitt, H. Huppertz, $Ni_6B_{22}O_{39}\cdot H_2O$ – extending the field of nickel borates, Z. Naturforsch. B: J. Chem. Sci. 72 (2017) 967-975. DOI: 10.1515/znb-2017-0148

[28] A. Sarkar, A. Dasgupta, B. Basu, A. Paul, Optical absorption of nickel(II) and mixed-alkali effect in K_2O-Li_2O-B_2O_3 glasses, J. Mater. Sci. Lett., 2 (1983), 697-700. DOI: 10.1007/BF00720406

[29] R.D. Shannon, Revised effective ionic radii and systematic studies of interatomic distances in halides and chalcogenides, Acta Crystallogr. A32 (1976) 751-767. DOI: 10.1107/S0567739476001551

[30] C.R. Ross, H. Keppler, D. Canil, H.St.C., O'Neill, Structure and crystal-field spectra of $Co_3Al_2(SiO_4)_3$ and $(Mg,Ni)_3Al_2(SiO_4)_3$ garnet, Amer. Miner. 81 (1996) 61–66. DOI: 10.2138/am-1996-1-209

[31] A. Paul, Activity of nickel oxide in alkali borate melts, J. Mater. Sci. 10 (1975) 422-426. DOI:10.1007/BF00543686

[32] B.W. White, G.J. McCarthy, B.E. Scheetz, Optical spectra of chromium, nickel, and cobalt-containing pyroxenes, Amer. Miner. 56 (1971) 72-89.

[33] C.A. Niedermeier, M. Råsander, S. Rhode, V. Kachkanov, B. Zou, N. Alford, M.A. Moram, Band gap bowing in $Ni_xMg_{1-x}O$, Sci. Rep. 6 (2016) 31230. DOI: 10.1038/srep31230

[34] C.P.C. Medrano, E. Sadrollahi, R.G.M. Da Fonseca, E.C. Passamani, D.C. Freitas, M.A. Continentino, D.R. Sanchez, F.J. Litterst, E. Baggio-Saitovitch, Magnetic properties of $Ni_5Sn(O_2BO_3)_2$ ludwigite, Phys. Rev.B 103 (2021) 064430. DOI: 10.1103/PhysRevB.98.054435

[35] S. Busche, K. Bluhm, Synthesis and Crystal Structure of the first zinc containing pyroborates $Ni_{1.5}Zn_{0.5}(B_2O_5)$ and $Co_{1.5}Zn_{0.5}(B_2O_5)$, Z. Naturforsch. 50b (1995) 1445-1449.

[36] M. Rubinstein, R. Kodama, S.A. Makhlouf, Electron spin resonance study of NiO antiferromagnetic nanoparticles, J. Magn. Magn. Mater. 234 (2001) 289-293. DOI: 10.1016/S0304-8853(01)00313-4

[37] R. Juza, H. Seidel, J. Tiedemann, Color centers in alkali borate glasses containing cobalt, nickel, or copper, Angew. Chem. Int. Ed. 5 (1966) 85-94. DOI: 10.1002/anie.196600851

[38] R. Kado, G. Lelong, L. Galoisy, D. Matsumura, G. Calas, T. Yano, Structural significance of nickel sites in aluminosilicate glasses, J. Non-Cryst. Solids 539 (2020) 120070. DOI: 10.1016/j.jnoncrysol.2020.120070

[39] X.A. Chen, M. Li, X.N. Chang, H.G. Zang, W.Q. Xiao, Synthesis and crystal structure of a novel pentaborate $Na_3ZnB_5O_{10}$, J. Solid State Chem. 180 (2007) 1658-1663. DOI: 10.1016/j.jssc.2007.03.014

[40] X. Chen, C. Yang, X. Chang, H. Zang, W. Xiao, Syntheses and characterization of two alkali-metal zinc borates, α-$LiZnBO_3$ and $Li_{0.48}Na_{0.52}ZnBO_3$, Solid State Sci. 11 (2009) 2086-2092 DOI: 10.1016/j.solidstatesciences.2009.08.024

[41] S. Tamilarasan, M.L.P. Reddy, S. Natarajan, J. Gopalakrishnan, Developing intense blue and magenta colors in α-$LiZnBO_3$: the role of 3d-metal substitution and coordination, Chem. Asian J. 11 (2016) 3234-3240. DOI: 10.1002/asia.201601124

[42] F. Strauss, G. Rousse, M.T. Sougrati, D.A.D. Corte, M. Courty, R. Dominko, J.M. Tarascon, Synthesis, structure, and electrochemical properties of $Na_3MB_5O_{10}$ (M= Fe, Co) containing M^{2+} in tetrahedral coordination, Inorg. Chem. 55 (2016) 12775-12782. DOI: 10.1021/acs.inorgchem.6b02070

[43] L. Cormier, D. Ghaleb, J.M. Delaye, G. Calas, Competition for charge compensation in borosilicate glasses: Wide-angle x-ray scattering and molecular dynamics calculations, Phys. Rev. B 61 (2000) 14495-14999. DOI: 10.1103/PhysRevB.61.14495

[44] W.H. Turner, J.A. Turner, Ligand□Field spectra and structure of nickel in silicate glasses, J. Am. Ceram. Soc. 55 (1972) 201-207. DOI: 10.1111/j.1151-2916.1972.tb11259.x

731 [45] S. Tamilarasan, S. Laha, S. Natarajan, J. Gopalakrishnan, Exploring the colour of 3d transition-metal
732 ions in trigonal bipyramidal coordination: identification of purple-blue (CoO_5) and beige-red (NiO_5)
733 chromophores in $LiMgBO_3$ host, Eur. J. Inorg. Chem. (2016) 288-293. DOI: 10.1002/ejic.201501064
734 [46] J.S. Knyrim, J. Friedrichs, S. Neumair, F. Roessner, Y. Floredo, S. Jakob, D. Johrendt, R. Glaum, H.
735 Huppertz, High-pressure syntheses and characterization of the transition metal borates beta-MB_4O_7 (M = Mn^{2+},
736 Ni^{2+}, Cu^{2+}), Solid State Sci. 10 (2008) 168-176. DOI: 10.1016/j.solidstatesciences.2007.09.004
737 [47] M.Á. Tena, R. Mendoza, C. Trobajo, J.R. García, S. García□Granda, $Co_2P_2O_7$–$Ni_2P_2O_7$ solid solutions:
738 structural characterization and color, J. Am. Ceram. Soc. 102 (2019) 3695-3704. DOI: 10.1111/jace.16158
739 [48] O.V. Livitska, N.Y. Strutynska, I.V. Zatovsky, N.S. Slobodyanik, The double phosphates $M^IM^{II}PO_4$ (M^I-
740 Na, K; M^{II} –Mg, Mn, Co, Ni, Zn)-synthesis from chloride melts and characterization, Cryst. Res. Technol. 50
741 (2015) 626-632. DOI: 10.1002/crat.201500028
742 [49] C. Thieme, T. Waurischk, C. Lin, C. Rüssel, Lilac ceramic pigments based on $Ba_{0.5}Sr_{0.5}Zn_{2x}Ni_xSi_2O_7$
743 solid solutions, Ceram. Int. 42 (2016) 13035-13040. DOI: 10.1016/j.ceramint.2016.05.082
744 [50] M. Gerloch, J. Kohl, J. Lewis, W. Urland, Single-crystal polarized spectrum and paramagnetic
745 anisotropy of five-co-ordinate square pyramidal nickel(II) complexes, J. Chem. Soc. A (1970) 3269-3283. DOI:
746 10.1039/J19700003269.
747 [51] J.F. Stebbins, Glass structure, melt structure, and dynamics: some concepts for petrology, Amer. Miner.
748 101 (2016) 753-768. https://doi.org/10.2138/am-2016-5386
749 [52] A. Graff, Z. Barrez, P. Baranek, M. Bachet, P. Bénézeth, Complexation of nickel ions by boric acid or
750 (poly)borates, J. Solut. Chem. 46 (2017) 25-43. DOI: 10.1007/s10953-016-0555-x
751 [53] W.J. Clarida, J.R. Berryman, M. Affatigato, S.A. Feller, S.C. Kroeker, J.W. Zwanziger, B. Meyer, F.
752 Borsa, S.W. Martin, Dependence of N4 upon alkali modifier in binary borate glasses, Phys. Chem. Glasses, 44
753 (2003) 215-217.
754 [54] V.K. Michaelis, P.M. Aguiar, S. Kroeker, Probing alkali coordination environments in alkali borate
755 glasses by multinuclear magnetic resonance, J. Non-Cryst. Solids 353 (2007) 2582-
756 2590. DOI: 10.1016/J.Jnoncrysol.2007.04.029

[55] T.C. Lin, C.A. Angell, Electronic spectra and coordination of Ni^{2+} in potassium borate glass and melt to 1000°C, J. Am. Ceram. Soc. 67 (1984) C33-C34. DOI:10.1111/j.1151-2916.1984.tb09618.x.

[56] L. Cormier, O. Majérus, D.R.s Neuville, G. Calas, Temperature-induced structural modifications between alkali borate glasses and melts, J. Am. Ceram. Soc. 89 (2006) 13-19. DOI: 10.1111/j.1551-2916.2005.00657.x

[57] P.S. Fiske, J.F. Stebbins, The structural role of Mg in silicate liquids: a high-temperature ^{25}Mg, ^{23}Na and ^{29}Si NMR study, Am. Mineral. 79 (1994) 848-861.

[58] L. Cormier, G. Calas, G. Cuello, Structural study of Ca–Mg and K–Mg mixing in silicate glasses by neutron diffraction, J. Non-Cryst. Solids 356 (2010) 2327-2331. DOI:10.1016/j.jnoncrysol.2010.02.023

[59] E.I. Kamitsos, M.A. Karakassides, G.D. Chryssikos, Vibrational spectra of magnesium-sodium-borate glasses. 2. Raman and mid-infrared investigation of the network structure, J. Phys. Chem. 9 (1987) 1073-1079. DOI:10.1021/acs.jpcc.8b09466

[60] H. Kawazoe, H. Kokumai, T. Kanazawa, Coordination of Mg2+ in oxide glasses determined by X-ray emission spectroscopy, J. Phys. Chem. Solids 42 (1981) 579-581

[61] G. Greaves, S. Sen, Inorganic glasses, glass-forming liquids and amorphizing solids, Adv Phys. 56 (2007) 1-166. DOI:10.1080/00018730601147426

[62] Y.D. Yiannopoulos, G.D. Chryssikos, E.I. Kamitsos, Structure and properties of alkaline earth borate glasses, Phys. Chem. Glasses, 42 (2001) 164-172.

[63] N. Bisbrouck, M. Bertani, F. Angeli, T. Charpentier, D. de Ligny, J.M. Delaye, S. Gin, M. Micoulaut, Impact of magnesium on the structure of aluminoborosilicate glasses: A solid-state NMR and Raman spectroscopy study, J. Am. Ceram. Soc. 104 (2021) 4518-4536. DOI:10.1111/jace.17876

[64] F.C. Hawthorne, A bond-topological approach to borate minerals: A brief review, Phys. Chem. Glasses, 59 (2018) 121-129. DOI:10.13036/17533562.59.3.023